이학석사학위논문

이광자 분광법을 이용한 과산화 아질산염에 대한 프로브

Probes for Peroxynitrite Using Two-Photon Microscopy

2016년 2월

서울대학교 대학원

화학부 유기화학전공

박 진 희

이광자 분광법을 이용한 과산화 아질산염에 대한 프로브

Probes for Peroxynitrite Using Two-Photon Microscopy

지도교수 홍 종 인

이 논문을 이학석사 학위논문으로 제출함

2016년 2월

서울대학교 대학원

화학부 유기화학전공

박 진 희

박 진 희의 이학석사 학위논문을 인준함

2015년 12월

위 원 장 **Soon Hyeok Hong** (인)

부위원장 홍 종 인 (인)

위 원 박 승 범 (인)

Probes for Peroxynitrite Using Two-Photon Microscopy

by

Jin-Hee Park

Supervisor: Prof. Jong-In Hong

A Thesis for the Master Degree
in Organic Chemistry

Department of Chemistry
Graduate School
Seoul National University

Probes for Peroxynitrite Using Two-Photon Microscopy

Abstract

Two-photon microscopy (TPM), utilizing two near-infrared (NIR) photons as the excitation source, has become a useful tool for biomedical research. However, only a few two-photon excitable probes for peroxynitrite have been developed that can detect peroxynitrite in various biological conditions using two-photon microscopy. However, two-photon peroxynitrite probe with an improved two-photon absorbing property is still required for further exploration.

Recently, it was reported that peroxynitrite can trigger oxidative N-dearylation reaction which can be used to induce fluorescence turn-on response. Thus, we have developed a new probe that can selectively detect peroxynitrite among other ROS/RNSs (Reactive oxygen/nitrogen species) utilizing dearylation reaction. The probe is highly selective and sensitive to peroxynitrite and has better two-photon excitation properties than any previous reported probes.

Further, we synthesized two-photon excitable lanthanide complexes to introduce unique properties of lanthanide phosphorescence- Sharp, line-like emission bands with the same fingerprint wavelengths and narrow peak widths, and long excited-state lifetimes in the ms~μs range. With further modification, these lanthanide based two-photon probes can be used to discover the effects of peroxynitrite in biological systems which are not clearly understood.

Keyword : Peroxynitrite, Two-Photon Microscopy, Fluorescence Probes, Lanthanide complexes

Student Number : 2013-22923

Contents

A. Background

A.1. Two-Photon Probes

Fluorescence imaging with small-molecule probes has become an important tool for studying living systems since they can detect targets rapidly with good selectivity and sensitivity, and can be easily loaded into cells. However, one-photon microscopy (OPM) utilizing one photon (OP) with short wavelength (350−550 nm) has several limitations for cell imaging and deep tissue imaging because the short wavelength of a photon can cause shallow penetration depth, autofluorescence and cell damage.[1]

Otherwise, two-photon microscopy (TPM), utilizing two near-infrared (NIR) photons (Figure 1) [2], has been used to image cells, tissues and animals. TPM has many advantages, such as localized excitation, reduced photodamage, longer observation time, and greater tissue penetration depth in comparison to OPM.[3,4,5,6] Therefore, various two-photon probes have been developed and their usability in bioimaging has been demonstrated.[7,8,9,10,11,12]

To show better properties of two-photon probes for biological target, probes should have a large two-photon absorption cross section (δ, in units of GM = 10^{-50} cm^4 s $photon^{-1}$ $molecule^{-1}$), which means the probability of a two-photon absorption (TPA) process. Probes with large δ values can be excited by lower laser power which can minimize photodamage. [1] Through many experiments, guidelines to design a probe with large δ values have been reported. The most important points of these guidelines is that enhancing the intramolecular charge transfer (ICT) produces an increase in the δ values

of the molecule. [13,14,15,16,17] Many two-photon probes are designed based on ICT enhancement. (Figure 2) [1]

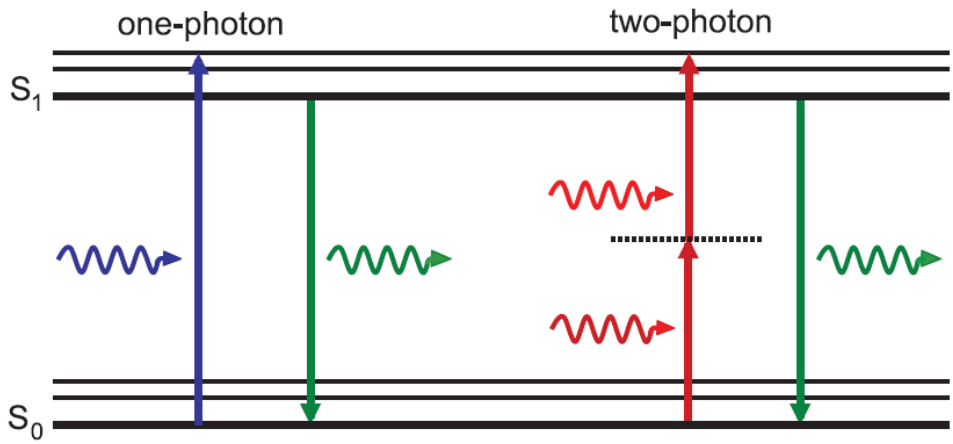

Figure 1. Concept of Two-photon excitation of fluorescence [2]

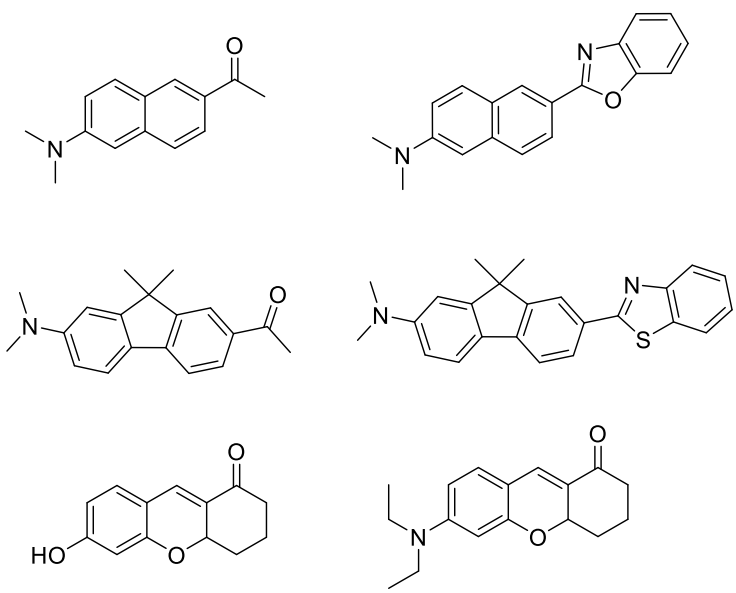

Figure 2. Representative two-photon fluorophores

A.2. Lanthanide-based Probes

Lanthanide based probes have been used widely in bioimaging because of the unique properties of lanthanide luminescence. The luminescence of lanthanides originates from the *f-f* electron transition in the *4f* subshell, which gives unique properties to the probe. First, the emissions of lanthanides are hardly affected by the surrounding environment and ligand field, since the 4f orbitals are shielded by 5s and 5p orbitals. Thus, lanthanide probes show sharp, line-like emission bands (the fingerprint wavelengths) whose wavelengths are constant regardless of the composing environments. Second, the luminescence has very long excited-state lifetime (ms to μs) because the *f-f* transitions are forbidden by the spin and Laporte rule.[18] This property allow lanthanide probes to image with time-resolved spectroscopy which can eliminate interferences caused by scattering and autofluorescence in biological conditions.

However, direct excitation of lanthanide complexes need very intense light sources because the *f-f* transition is forbidden. Thus, most lanthanide probes use a sensitizer (antenna), which can absorb the excitation light and sensitize the lanthanide ions (Figure 3). [19] When a sensitizer is excited by a light source, the singlet excited state of the sensitizer undergoes an intersystem crossing to the triplet excited state. Then, energy transfer occurs from the triplet excited state of the sensitizer to the emissive excited state of the lanthanide (sensitization). When sensitization occurs, the energy level of the triplet state of the sensitizer should be at least 1850 cm^{-1} higher than that of emissive excited state of the lanthanide.[20] If the energy gap is less than 1850 cm^{-1}, back energy transfer from the emissive excited state of the lanthanide to the triplet state of

the sensitizer can take place. This gives a long life time of the triplet excited state of the sensitizer, which can be quenched by O_2.

This O_2-effect can reduce the emission quantum yield. Therefore, the energy level of the triplet excited state of the sensitizer should be considered to design the lanthanide-based probe (Figure 4). [19] Reaction-based lanthanide probes induce the change of luminescence intensity by using a sensitizer whose structures are altered through the reaction with a target (Figure 5). [21]

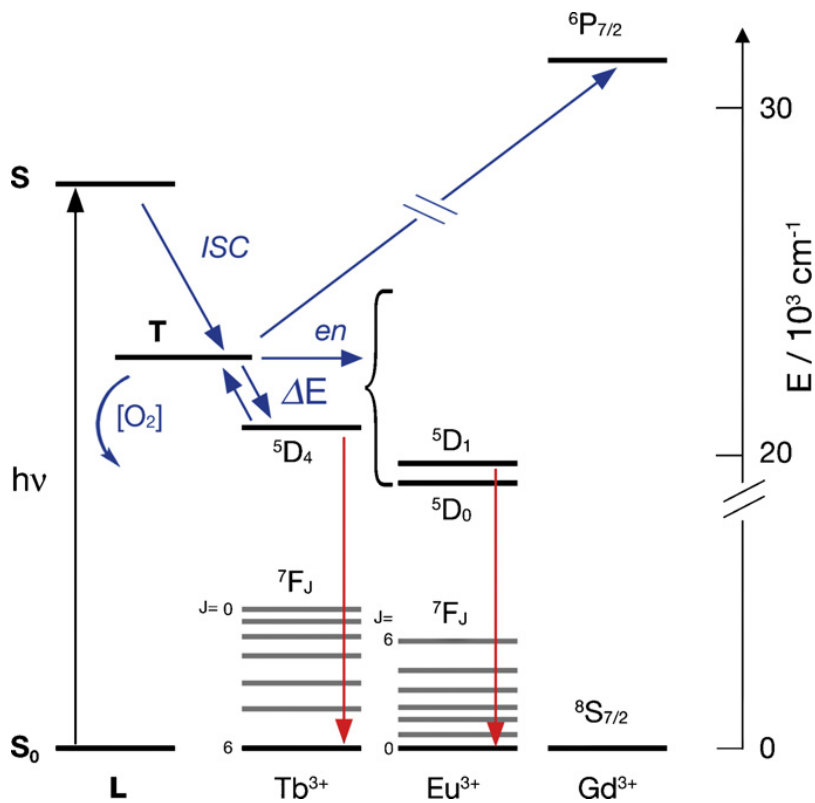

Figure 3. Sensitization of the luminescence in some lanthanide cations; blue arrows indicate non-radiative processes, red arrows indicate radiative processes.[19]

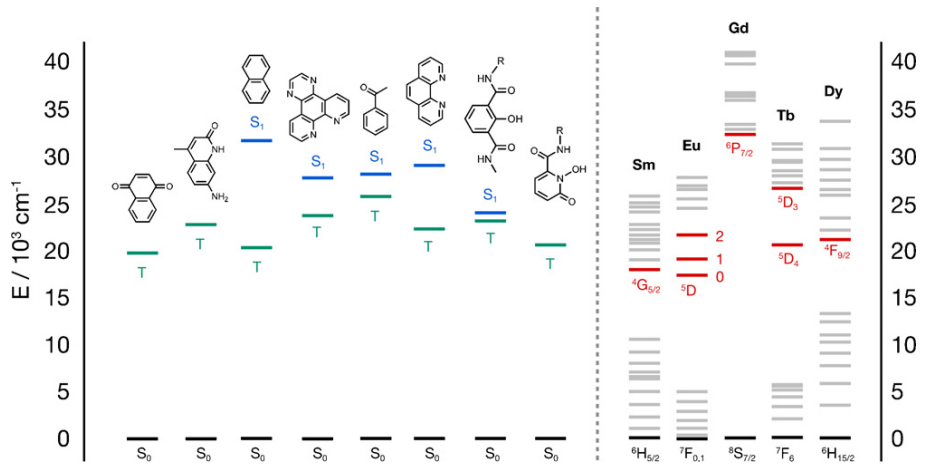

Figure 4. Energy diagram of the emissive levels of some lanthanide cations and sensitizers [19]

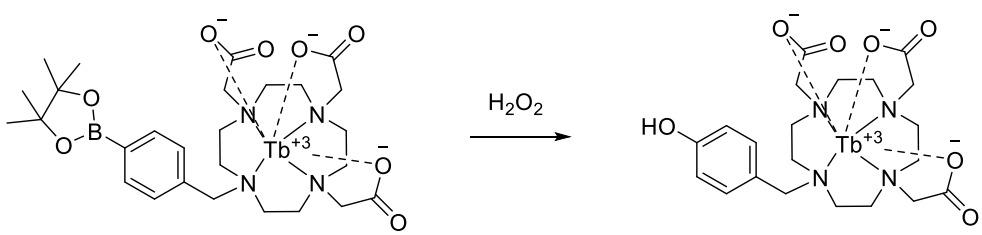

Figure 5. Lanthanide based hydrogen peroxide probe.

To develop efficient lanthanide based probes, coordinating ligand should be considered. Coordinating ligand should chelate lanthanide and protect the lanthanide ion from solvent coordination. Solvent coordination can cause vibrational energy transfer from the excited state of the lanthanide ion to the high-frequency X−H (X = C, N, O) oscillator, which shorten the lifetime of the excited state of the lanthanide (Figure 6). [22] Thus, chelating ligand should coordinate tightly with large coordination numbers in order to exclude as many vibrational oscillators from the lanthanide ion as possible.

Some lanthanide-based probes get turn-on responses from the change of the coordination number (Figure 7). [23] The lanthanide probe (Figure 7) shows increased emission intensity only when bicarbonate is coordinated to the lanthanide ion displacing the water molecules.

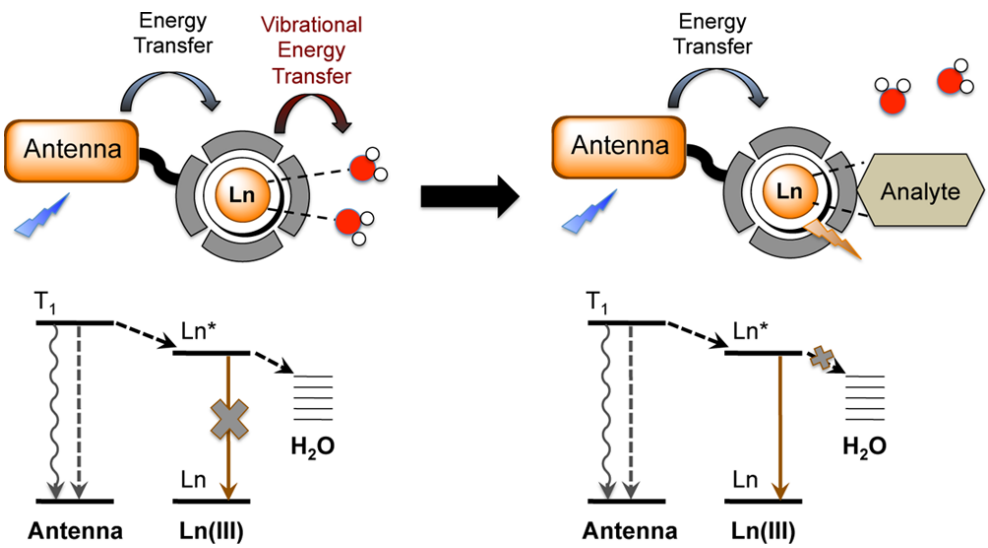

Figure 6. General scheme for the luminescence of lanthanide depending on the number of bound solvent (water) molecules. [22]

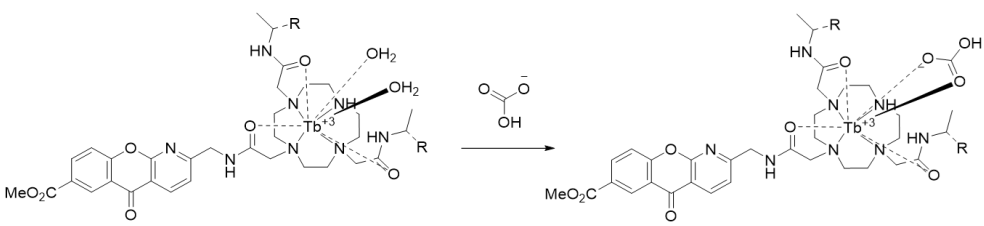

Figure 7. Bicarbonate-selective complexes that localize in the mitochondria

A.3. Luminescence probes for peroxynitrite

Peroxynitrite ($ONOO^-$) formed by the reaction between NO and $O_2^{\bullet-}$ is a strong oxidant found in biological system. $ONOO^-$ causes oxidation and nitration of biomolecules that are involved in a variety of physiological and pathological processes.[24] $ONOO^-$ plays important roles in immune responses against invading pathogens or cancer cells and redox regulation of signaling pathways.[25,26] However, $ONOO^-$ is also related to many diseases, such as cardiovascular, neurodegenerative, inflammatory and metabolic diseases, and pain, and cancer.[27]

However, the physiological roles of $ONOO^-$ are so far ambiguous due to its short half-life (<20 ms) and low concentration in the cells of living organisms. Therefore, development of new chemical tools for detecting peroxynitrite has been highly demanded.

Luminescence probes for peroxynitrite have been vigorously developed, and are able to detect $ONOO^-$ directly in cells. Most luminescence probes are designed as reaction-based probes whose targeting moieties are trifluorocarbonyl[28], phenyl boronic ester[29], hydrazine[30], selenium[31], nitrative aromatic ring[32] and electron-rich aromatic rings[33, 34].

A.4. References

[1] Kim, H. M.; Cho, B. R. *Chem. Rev.* **2015**, *115*, 5014−5055

[2] Benninger, R. K.; Piston, D. W. *Current Protocols in Cell Biology*. **2013**, *59*, 4.11.1–4.11.24.

[3] Helmchen, F.; Denk, W. *Nat. Methods*, **2005**, *2*, 932–940.

[4] (a) Kim, H. M.; Cho, B. R. *Acc. Chem. Res.* **2009**, *42*, 863–872; (b) Yao, S.; Belfield, K. D. *Eur.*

J. Org. Chem. **2012**, 3199–3217; (c) Liu, F.; Wu, T.; Cao, J.; Cui, S.; Yang, Z.; Qiang, X.; Sun, S.; Song, F.; Fan, J.; Wang, J. ; Peng, X.; *Chem. – Eur. J.* **2013**, *19*, 1548–1553; (d) Li, L.; Zhang, C. W.; Chen, G. Y.; Zhu, B.; Chai, C.; Xu, Q. H.; Tan, E. K.; Zhu, Q.; Lim, K. L.; Yao, S. Q. *Nat. Commun.* **2014**, *5*, 3276; (e) Dong, X.; Heo, C. H.; Chen, S.; Kim, H. M.; Liu, Z. *Anal. Chem.* **2014**, *86*, 308–311; (f) Zhou, L.; Zhang, X.; Wang, Q.; Lv, Y.; Mao, G.; Luo, A.; Wu, Y.; Wu, Y.; Zhang, J.; Tan, W. *J. Am. Chem. Soc.* **2014**, *136*, 9838–9841.

[5] (a) Bae, S. K.; Heo, C. H.; Choi, D. J.; Sen, D.; Joe, E. H.; Cho, B. R.; Kim, H. M. *J. Am. Chem. Soc.* **2013**, *135*, 9915–9923; (b) Kim, H. J.; Heo, C. H.; Kim, H. M. *J. Am. Chem. Soc.* **2013**, *135*, 17969–17977.

[6] (a) Lee, H.W.; Heo, C. H.; Sen, D.; Byun, H. O.; Kwak, I. H.; Yoon, G.; Kim, H. M. *Anal. Chem.* **2014**, *86*, 10001–10005; (b) Li, L.; Shen, X.; Xu, Q. H.; Yao, S. Q. *Angew. Chem., Int. Ed.* **2013**, *52*, 424–428; (c) Li, L.; Ge, J.; Wu, H.; Xu, Q. H.; Yao, S. Q. *J. Am. Chem. Soc.* **2012**, *134*, 12157–12167.

[7] Kim, H. M.; Cho, B. R. *Acc. Chem. Res.* **2009**, *42*, 863.

[8] Kim, H. M.; Cho, B. R. *Chem.-Asian J.* **2011**, *6*, 58.

[9] Sumalekshmy, S.; Fahrni, C. J. *Chem. Mater.* **2011**, *23*, 483.

[10] Yao, S.; Belfield, K. D. *Eur. J. Org. Chem.* **2012**, 3199.

[11] Kim, H. M.; Cho, B. R. *Oxid. Med. Cell. Longevity* **2013**, *2013*, 1−11.

[12] Kim, D.; Ryu, H. G.; Ahn, K. H. *Org. Biomol. Chem.* **2014**, *12*, 4550.

[13] Rumi, M.; Barlow, B.; Wang, J.; Perry, J. W.; Marder, S. R. *Adv. Polym. Sci.* **2008**, *213*, 1−95.

[14] Strehmel, B.; Strehmel, V. *Adv. Photochem*. **2007**, *27*, 111−354.

[15] Pawlicki, M.; Collins, H. A.; Denning, R. G.; Anderson, H. L. *Angew. Chem., Int. Ed.* **2009**, *48*, 3244.

[16] Belfield, K. D.; Yao, S.; Bonder, M. V. *Adv. Polym. Sci*. **2008**, *213*, 1−95.

[17] He, G. S.; Tan, L. S.; Zheng, Q.; Prasad, P. N. *Chem. Rev*. **2008**, *108*, 1245.

[18] Bünzli, J.-C. G.; Chauvin, A.-S.; Kim, H. K.; Deiters, E.; Eliseeva, S.V. *Coord. Chem. Rev*. **2010**, *254*, 2623.

[19] Armelaoa, L.; Quicib, S.; Barigelletti, F.; Accorsic, G.; Bottarod, G.; Cavazzinib, M.; Tondelloe, E. *Coord. Chem. Rev*. **2010**, *254*, 487

[20] Latva, M.; Takalo, H.; Mukkala, V.-M.; Matachescu, C.; Rodriguez-Ubis, J.C.; Kankare, J.; *J. Lumin*. **1997**, *75*,149.

[21] (a) Terai, T.; Kikuchi, K.; Iwasawa, S.-Y.; Kawabe, T.; Hirata, Y.; Urano, Y.; Nagano, T. *J. Am.*

Chem. Soc. **2006**, *128*, 6938; (b) Pershagen, E.; Nordholm, J.; Borbas, K. E. *J. Am. Chem. Soc.* **2012**, *134*, 9832; (c) Lippert, A. R.; Gschneidtner, T.; Chang, C. J. *Chem. Commun.* **2010**, *46*, 7510.

[22] Heffern, M. C.; Matosziuk, L. M.; Meade, T. J. *Chem. Rev.* **2014**, *114* , 4496–4539

[23] (a) Smith, D. G.; McMahon, B. K.; Pal, R.; Parker, D. *Chem. Commun.* **2012**, *48*, 8520; (b) McMahon, B. K.; Pal, R.; Parker, D. *Chem. Commun.* **2013**, *49*, 5363; (c) Smith, D. G.; Pal, R.; Parker, D. *Chem.-Eur. J.* **2012**, *18*, 11604.

[24] Koppenol, W. H.; Moreno, J. J.; Pryor, W. A.; Ischiropoulos, H.; Beckman, J. S. *Chem. Res. Toxicol.* **1992**, *5*, 834−842.

[25] (a) Radi, R. *J. Biol. Chem*. **2013**, *288*, 26464. (b) Liaudet, L.; Vassalli, G.; Pacher, P. *Front Biosci*. **2009**, *14*, 4809.

[26] (a) MacMicking, J.; Xie, Q. W.; Nathan, C. *Annu. Rev. Immunol.* **1997**, *15*, 323−350; (b) Bogdan, C. *Nat. Immunol*. **2001**, *2*, 907−916; (c) Chakravortty, D.; Hensel, M. *Microbes Infect.* **2003**, *5*, 621−627.

[27] (a) Pacher, P.; Beckman, J. S.; Liaudet, L. *Physiol. Rev.* **2007**, *87*, 315. (b) Szabo, C.; Ischiropoulos, H.; Radi, R. *Nat. Rev. Drug Discovery*, **2007**, *6*, 662. (c) Ferrer-Sueta, G.; Radi, R. *ACS Chem. Biol.* **2009**, *4*, 161.

[28] Peng, T.; Yang, D. *Org. Lett.* **2010**, *12*, 4932−4935.

[29] Chen, Z.-J.; Ren, W.; Wright, Q. E.; Ai, H.-W. *J. Am. Chem. Soc.* **2013**, *135*, 14940−14943

[30] Ambikapathi, G.; Kempahanumakkagari, S. K.; Lamani, B. R.; Shivanna, D. K.; Maregowda, H. B.; Gupta, A.; Malingappa, P. *J. Fluoresc*. **2013**, *23*, 705−712.

[31] Yu, F.; Li, G.; Zhao, G.; Chu, T.; Han, K. *J. Am. Chem. Soc.* **2011**, *133*, 11030−11033

[32] Ueno, T.; Urano, Y.; Kojima, H.; Nagano, T. *J. Am. Chem. Soc.* **2006**, *128*, 10640−1064

[33] Peng, T.; Wong, N.; Chen, X.; Chan, Y.; Ho, D.H.; Sun, Z.; Hu, J.J.; Shen, J.; El-Nezami, H.; Yang, D. *J. Am. Chem. Soc.* **2014**, *136*, 11728−11734

[34] Zhang, Q.; Zhang, N.; Long, Y.; Qian, X.; Yang, Y. *Bioconjugate Chem.* Article ASAP, DOI: 10.1021/acs.bioconjchem.5b00396

B. Two-Photon Probes for Peroxynitrite

B.1.Two-Photon turn-on probe for peroxynitrite

B.1.1. Introduction

Different types of luminescence probes have been developed to detect intracellular peroxynitrite directly. However, these probes are excited by photons with short wavelengths (from UV to visible light), thus limiting their use in cells and tissues due to autofluorescence, artificial reactive oxygen species (ROS) generation, and shallow penetration. [1]

Two-photon microscopy (TPM) utilizes two photons with a long wavelength (near infrared) for excitation. TPM has been used for biomedical research. TPM has many advantages such as localized excitation, low photodamage, and deep penetration depth. [2, 3, 4] Nonetheless, only a few two-photon excitable probes for $ONOO^-$ were reported.[5] These types of probes detected peroxynitrite in live cells and tissues using two-photon microscopy. However, a two-photon peroxynitrite probe with an advanced two-photon absorbing property is highly required for further investigation of $ONOO^-$.

In this thesis, we report a noble peroxynitrite probe (**JH-PN4**) that shows good selectivity among other ROS/RNSs (Reactive oxygen/nitrogen species) by utilizing a peroxynitrite-triggerd dearylation reaction.[5b] **JH-PN4** can also detect $ONOO^-$ in nanomolar concentration levels and have better two-photon excitation properties than previous reported probe. [5a]

B.1.2. Results and Discussion

Design of Probes

The **JH-PN4** is composed of 2-methylamino-6-acetylnaphthalene (acedan), a well-known two-photon fluorophore, as a reporting group [6] and N-methyl-*p*-hydroxyaniline as a targeting moiety. The N-phenyl group quenching the fluorescence of 2-methylamino-6-acetylnaphthalene can be eliminate efficiently by $ONOO^-$ with good selectivity among other ROS/RNSs. [5b] Dearylation can make the fluorescence of acedan recovered through making the probe have "push-pull" structure (Scheme 1A). In addition, we also synthesized probes **JH-PN1~JH-PN3** in order to investigate the N-, O- substituents effects. (Scheme 1B).

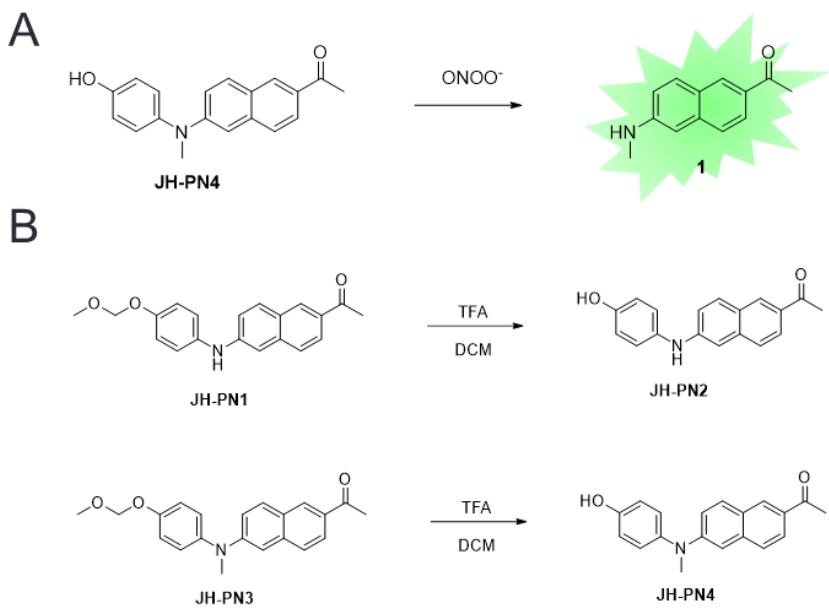

Scheme 1. (A) Sensing mechanism and (B) structures of **JH-PN1~4**. TFA = trifluoroacetic acid, DCM = dichloromethane.

Selectivity tests of JH-PN1~4

With **JH-PN1~4**, we performed a selectivity test for $ONOO^-$ among other ROS/RNSs in 10 mM phosphate-buffered saline (PBS) solution (0.4% DMF, pH 7.4). As expected, **JH-PN1, JH-PN3**, having a methoxymethyl ether group did not give any remarkable response to the $ONOO^-$ and other ROS species (Figures 1A and 1C). Also, **JH-PN2** composed of the diarylamino (Ar-NH-Ar′) group, show only slight increase in

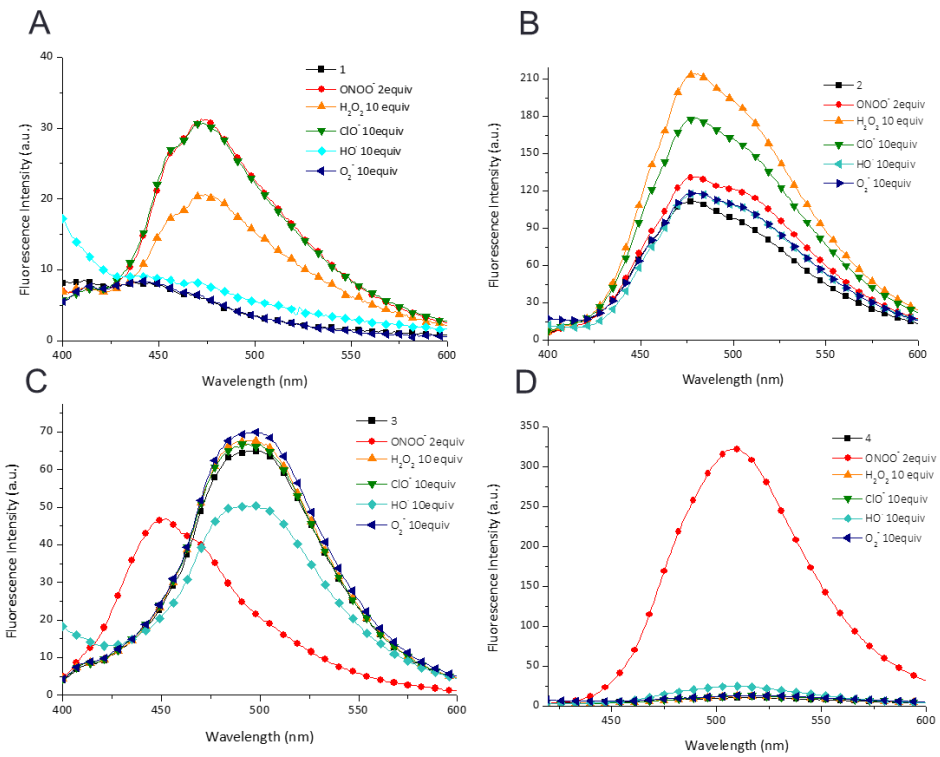

Figure 1. Fluorescence spectra of (A) **JH-PN1** (B) **JH-PN2** (C) **JH-PN3** (D) **JH-PN4** (20 μM) with various ROS/RNSs. (2.0 equiv. for $ONOO^-$, 10 equiv. for other ROSs). Data were acquired at 25 ℃ in 10 mM phosphate buffer with 0.4% dimethyl formamide (DMF) at pH 7.4 with excitation at 360 nm. Reaction were carried out for 1h at room temperature before the fluorescence intensity of the probe solutions was measured.

the fluorescence intensity upon the addition of $ONOO^-$ or other species (Figure 1B). This is probably due to the oxidation of diarylamine by the $ONOO^-$.[7]

Otherwise, the fluorescence intensity of **JH-PN4** at 509 nm was increased more than 32-fold when 2 equiv. of $ONOO^-$ were added. Moreover, any significant change was not observed with other excess ROS/RNSs (Figure 2). Although a slight increase of fluorescence intensity was observed with nitric oxide (NO), it is negligible because the amount of NO added to the probe was too large (2 mM) which cannot exist in the cells. In addition, fluorescence change with NO is much smaller than that with $ONOO^-$. Therefore, **JH-PN4** was chosen for the next experiments.

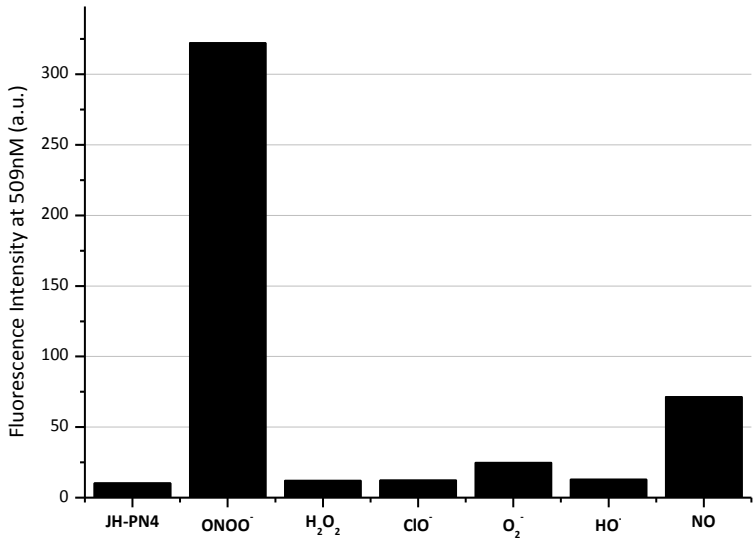

Figure 2. Fluorescence Intensity (λ_{em} = 509 nm) of **JH-PN4** (20 μM) with various reactive oxygen/nitrogen species [ROS/RNSs, 2.0 equiv. for $ONOO^-$, 10 equiv. for other ROSs, and 100 equiv. for nitric oxide (NO)]. Data were acquired at 25 ℃ in 10 mM phosphate buffer with 0.4% dimethyl formamide (DMF) at pH 7.4 with excitation at 360 nm. Reactions were carried out for 1h at room temperature before the fluorescence intensity of the probe solutions was measured.

Fluorescence response of JH-PN4

First, to test the sensitivity of **JH-PN4**, fluorescence change was measured with increasing concentrations of $ONOO^-$ (Figure 3). The fluorescence intensity of **JH-PN4** at 509 nm increased more than 57-fold with the addition of 5 equiv. of $ONOO^-$ (Figure 3A). This is due to the removal of the N-phenyl group, which quenches the

fluorescence of the probe, by dearylation. The detection limit of **JH-PN4** was estimated to be as low as 359 nM (Figure 3B, and 4), confirming a high sensitivity of **JH-PN4** to $ONOO^-$. However, the fluorescence intensity decreased with more than 5 equiv. of $ONOO^-$. These results probably arose from further oxidation of acedan produced by dearylation of **JH-PN4** with $ONOO^-$. The secondary amine group of acedan can be oxidized with excess $ONOO^-$, reducing the fluorescence of acedan. [5b, 7]

Then, we investigated the time-dependent fluorescence change of **JH-PN4** with 1 equiv. of $ONOO^-$ (Figure 5). **JH-PN4** showed a rapid turn-on response to $ONOO^-$ within 3s and the reaction was saturated within 10min (Figure 5B) proving that **JH-PN4** can rapidly detect $ONOO^-$ whose life time in intracellular condition is very short.

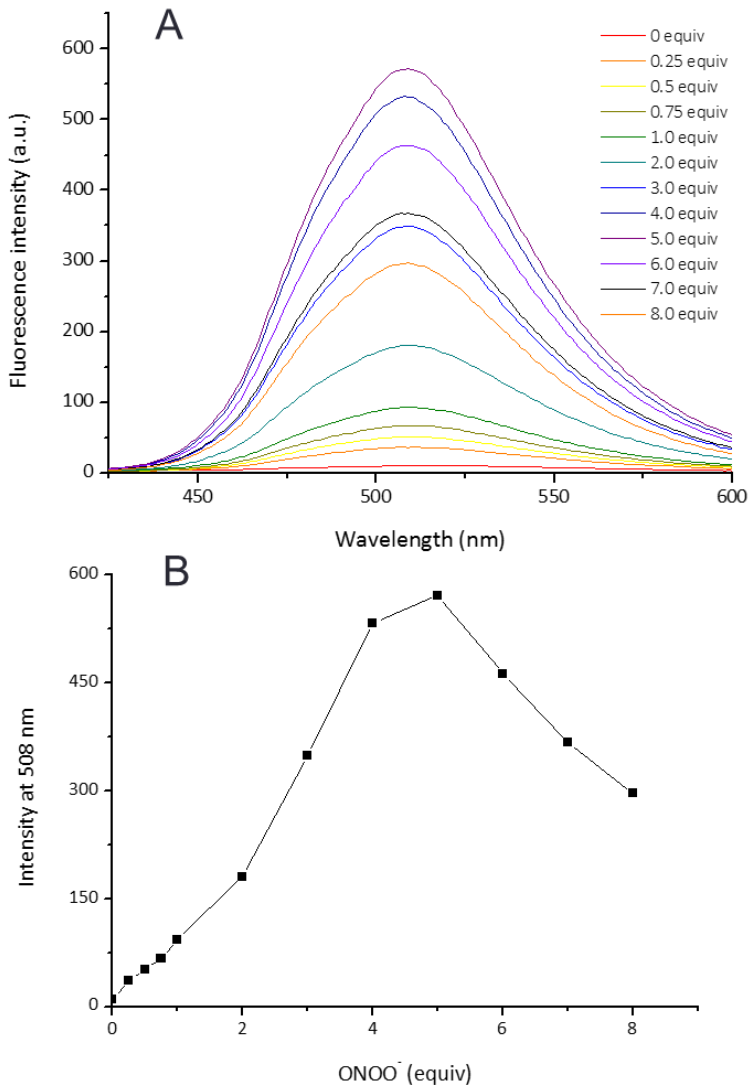

Figure 3. Testing the sensitivity of **JH-PN4**: (A) fluorescence spectra and (B) fluorescence intensity at 508 nm of **JH-PN4** (20 μM) with $ONOO^-$ (0~8 equiv.). Data were acquired at 25 ℃ in 10 mM phosphate buffer with 0.4% dimethyl formamide (DMF) at pH 7.4 with excitation at 360 nm. Reactions were carried out for 30 min at room temperature before the fluorescence intensity of the probe solutions was measured.

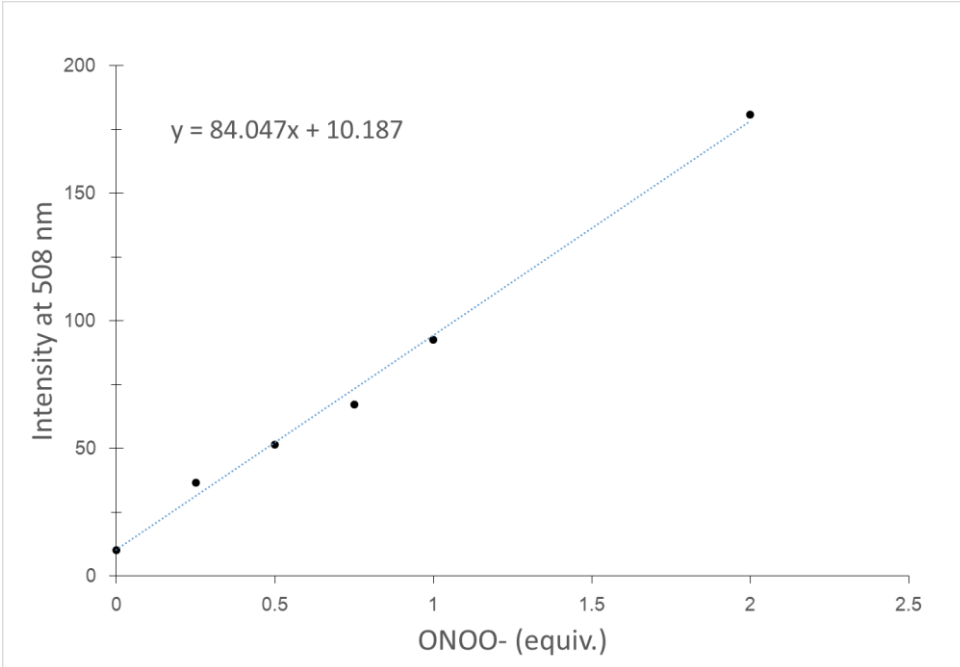

Figure 4. Linear plot of the fluorescence intensity at 508 nm of **JH-PN4** (20 μM) against a $ONOO^-$ concentration. Data were acquired at 25 ℃ in 10 mM phosphate buffer with 0.4% dimethyl formamide (DMF) at pH 7.4 with excitation at 360 nm. Reactions were carried out for 30 min at room temperature before the fluorescence intensity of the probe solutions was measured.

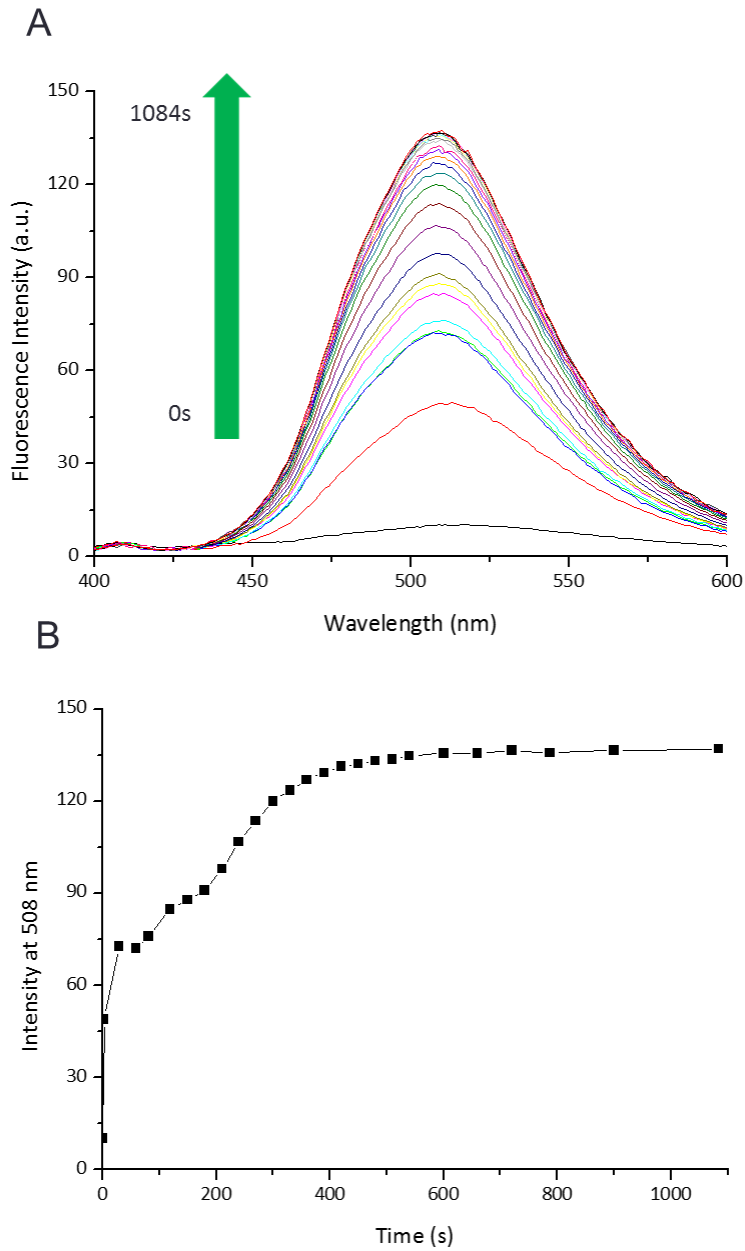

Figure 5. (A) Time-dependent fluorescence change and (B) time course of fluorescence Intensity (λem = 509 nm) of **JH-PN4** (10 μM) in 10 mM phosphate buffer saline (PBS) (0.2% DMF, pH 7.4) in the presence of 1.0 equiv. $ONOO^-$ (λ_{ex} = 360 nm).

Next, we measured the fluorescence change of **JH-PN4** with $ONOO^-$ using two-photon excitation mode (Figure 6). As expected, **JH-PN4** showed fluorescence turn-on response to $ONOO^-$ with two-photon excitation (Figure 6A). A maximum two-photon absorption cross section (σ_{max}) of **JH-PN4** with 3 equiv. of $ONOO^-$ was 8.8 GM at 740 nm which is an improved value when compared with previous reported probes.[5a] In addition, the value of a two-photon action cross section increased about 4 times with 3 equiv. of $ONOO^-$ (Figure 6B).

Effect of pH to Fluorescence of Probe 4

To test the availability of **JH-PN4** as a $ONOO^-$ probe, the fluorescence intensities of **JH-PN4** and product **1** was observed in a PBS with different pH values ranging from 4 to 9 (Figure 7). A noticeable change was not observed in various pH conditions. The fluorescence intensity of **JH-PN4** at 509 nm slightly increased in basic conditions (> pH 9), but was insignificant when compared to the change of fluorescence intensity with the addition of $ONOO^-$. Moreover, the fluorescence intensity of product **1** reduced at pH 4, which is also trivial. This suggests that **JH-PN4** is very stable in a range of pH conditions and is usable in a physiological condition.

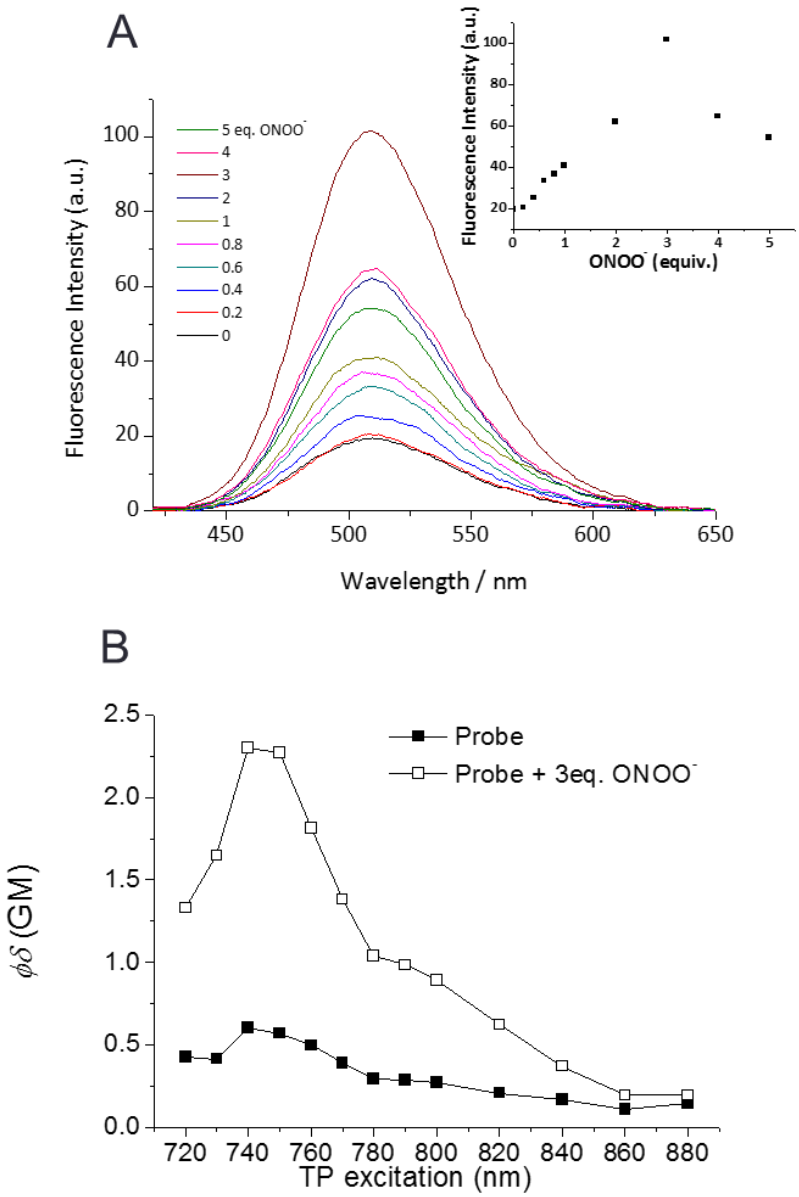

Figure 6. (A) Two-photon fluorescence spectra of **JH-PN4** (10 μM) with $ONOO^-$. Inset shows Two-photon fluorescence titration curve for **JH-PN4** with $ONOO^-$. The excitation wavelength was 740 nm. (B) Two-photon action spectra of **JH-PN4** in the absence (■) and in the presence of $ONOO^-$ (□). These data were measured in 10 mM phosphate buffer saline (PBS).

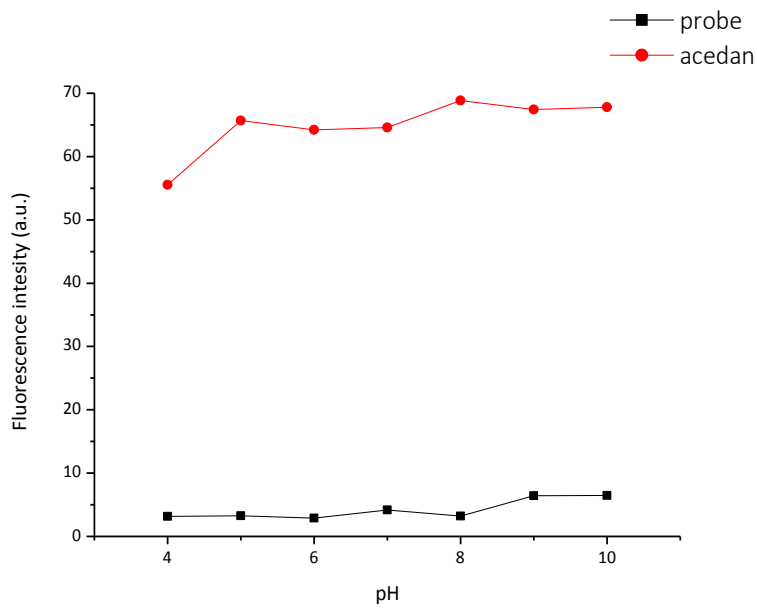

Figure 7. Fluorescence intensities at 509 nm of **JH-PN4** and **1** (10 μM) at various pH values. (λ_{ex} = 360 nm)

Live cell imaging

We tested the ability of **JH-PN4** to image $ONOO^-$ in live cells by two-photon microscopy. With SIN-1 (3-morpholinosydnonimine hydrochloride), exogenous $ONOO^-$ donor, (Figure 8) and endogenous $ONOO^-$, (Figure 9) intracellular fluorescence increased slightly. However, they were too small to overcome error range. (Figure 8B and 9B) It can be assumed that dearylation of the N-phenyl group in **JH-PN4** does not vigorously occurred compared with other probes.[5] The fact that the maximum fluorescence intensity of **JH-PN4** with $ONOO^-$ in fluorescence titration (Figure 3) is

much smaller than the estimated fluorescence intensity of product **1** support this assumption.

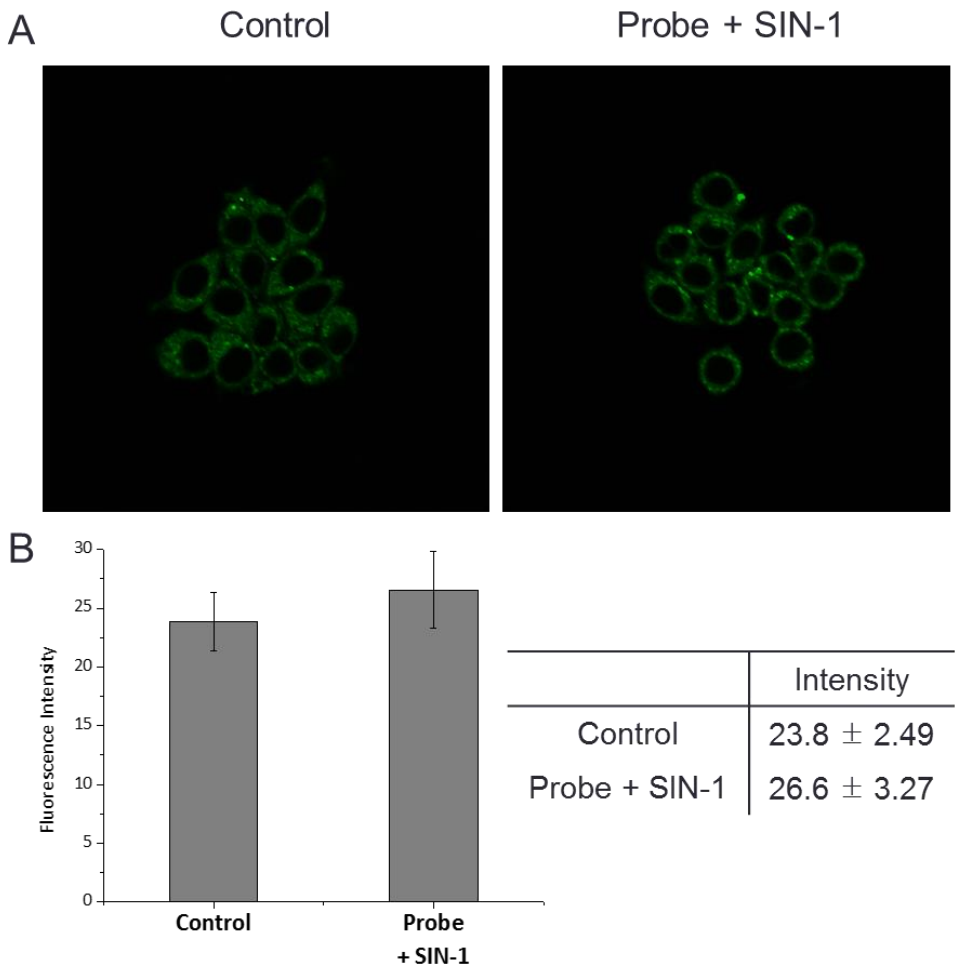

Figure 8. (A) Two-photon microscopy images of exogenous $ONOO^-$ donor with **JH-PN4** in RAW 264.7 macrophages. (B) Quantification of the fluorescence signals from (A). Cells were pre-treated with SIN-1 (10 μM) for 10 min, and then incubated with **JH-PN4** (10 μM) for 30 min. The intensities were collected at 400-600 nm upon excitation at 740 nm.

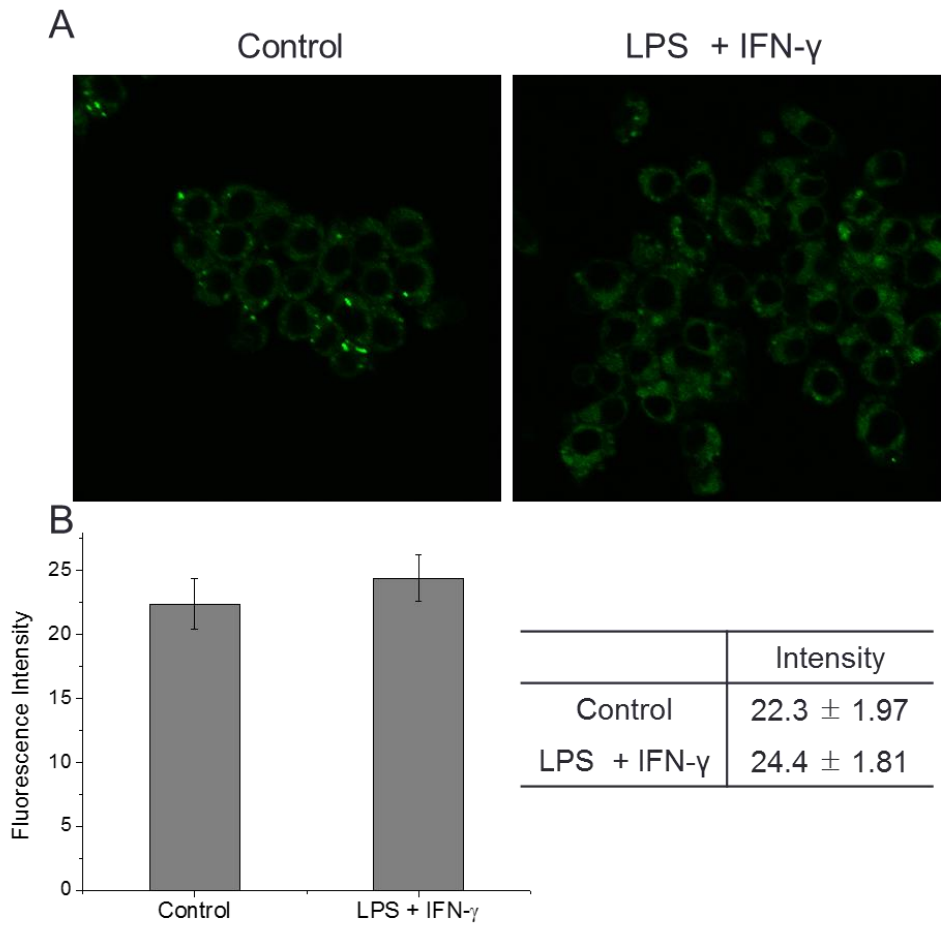

Figure 9. Two-photon microscopy images of endogenous $ONOO^-$ with **JH-PN4** in RAW 264.7 macrophages. Cells were pre-treated with LPS (1 μg/ml) and IFN-γ (100 ng/ml) for 14 h, and then incubated with **JH-PN4** (10 μM) for 30 min. The intensities were collected at 400-600 nm upon excitation at 740 nm.

B.1.3. Conclusion

We developed a two-photon turn-on probe for peroxynitrite using peroxynitrite-triggered dearylation. **JH-PN4** is a highly sensitive and selective probe for peroxynitrite among other ROS/RNSs and has improved two-photon excitation properties in comparison with previous reported probes. Thus, we imaged intracellular peroxynitrite with **JH-PN4,** but fluorescence increase was too small in cellular conditions. In the future research, further modification to increase the reactivity of targeting moiety should be conducted to develop useful tools for imaging cellular peroxynitrite.

B.1.4. Experimental Section

Synthesis and characterization of probes

All the chemicals were purchased from commercial suppliers and used without further purification except anhydrous solvents. Reactions were monitored by thin layer chromatography with Merck silica gel 60 F254 on aluminum foil. Merck silica gel 60 was used as stationary phase for column chromatography. Celite® 545 was used for filtration. All the ^{1}H and ^{13}C NMR spectra were recorded on Bruker DRX 300 NMR spectrometer. Fluorescence emission spectra were recorded with a JASCO FP-6500 spectrometer and the slit width was 3 or 10 nm for excitation and 3 or 5 nm for emission. HRMS data were obtained from Agilent 6890 Series, with FAB positive

mode. Following figure is synthetic scheme for probes. (TEA = trimethylamine, Tf_2O = trifluoromethanesulfonic anhydride, dba = dibenzylideneacetone, BINAP = (±) 2,2'-bis(diphenylphosphino)-1,1'-binaphthyl, TFA = trifluoroacetic acid, DCM = dichloromethane.)

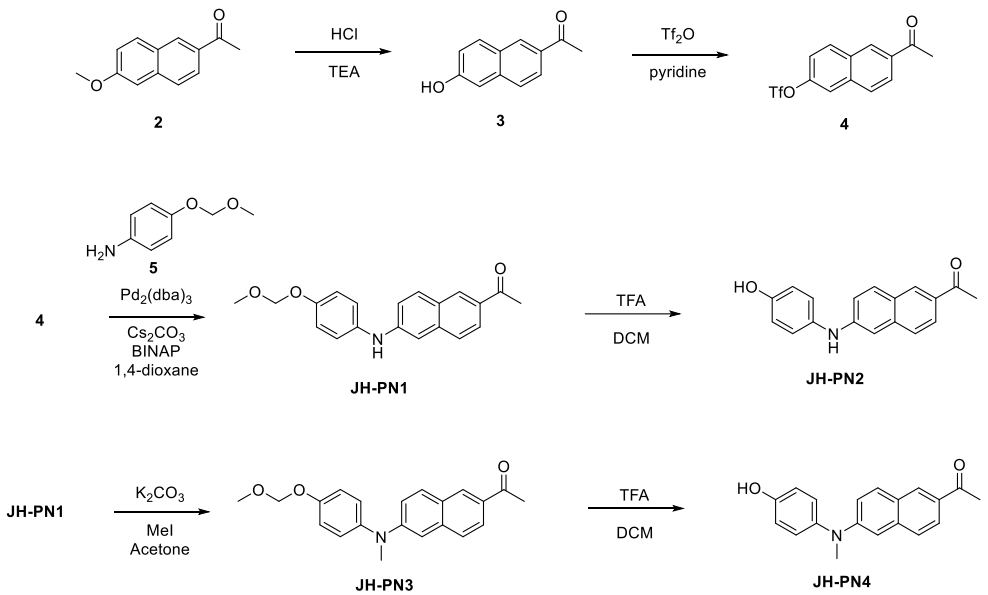

Compound **4** [5b] and **5** [8] were prepared by the literature method and synthesis of the other compounds is described below.

Synthesis of **JH-PN1**

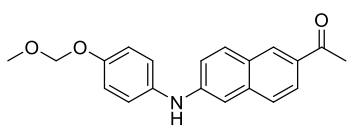

JH-PN1

A round bottom flask was charged with $Pd_2(dba)_3$ (0.05 equiv.), BINAP (0.15 equiv.) and Cs_2CO_3 (1.4 equiv.), and flushed with N_2 gas for 5 min. A solution of **4** (4.33 g, 13.6 mmol) and **5** (1.2 equiv.) in dioxane (10 ml) was added, and the resulting mixture was

first stirred under N_2 atmosphere at room temperature for 30 min and then at 100 ℃ for 20 h. At that time the reaction mixture was allowed to cool to room temperature, diluted with CH_2Cl_2 and filtered through a pad of Celite. The filter cake was washed with CH_2Cl_2. The filtrate was then concentrated and the residue was purified by silica gel column chromatography using CH_2Cl_2 as the eluent to give **JH-PN1** in 63.4% yield. ^{1}H NMR (300 MHz, $CDCl_3$): δ 8.35 (s, 1H), 7.89 (dd, J = 38.3, 7.7 Hz, 2H), 7.61 (d, J = 8.2 Hz, 1H), 7.22 – 7.10 (m, 6H), 5.89 (s, 1H), 5.21 (s, 2H), 3.55 (s, 3H), 2.70 (s, 3H); ^{13}C NMR (75.47 MHz, $CDCl_3$): δ 197.81, 153.68, 145.41, 137.55, 135.35, 131.64, 131.09, 130.24, 127.02, 126.35, 124.79, 123.29, 119.11, 117.48, 107.38, 94.91, 56.04, 26.50. HRMS (FAB^+) [M=$C_{20}H_{19}NO_3$], calculated 321.1365, found 321.1365.

Synthesis of **JH-PN2**

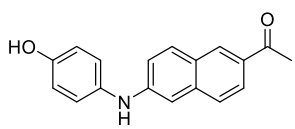

JH-PN2

To a solution of **JH-PN1** (321 mg, 1 mmol) in dry CH_2Cl_2 (5 ml), trifluoroacetic acid (5 ml) was added dropwise at 0 ℃. The resulting solution was stirred at room temperature until TLC indicated that all starting materials were consumed. The mixture was then concentrated in vacuo and azeotroped with toluene three times to give compound **JH-PN2**. The crude product was then purified by silica gel column chromatography using Hexane/EtOAc (4:1) as eluent to give **JH-PN2** in 99% yield. ^{1}H NMR (300 MHz, $CDCl_3$): δ 8.30 (s, 1H), 7.97 (dd, J = 19.5, 8.9 Hz, 2H), 7.50 (d, J = 8.9 Hz, 1H), 6.87 (d, J = 8.9 Hz, 2H), 6.63 – 6.56 (m, 4H), 5.77 (s, 1H), 4.83 (s, 1H),

2.66 (s, 3H); ^{13}C NMR (75.47 MHz, DMSO-d_6): δ 197.83, 153.76, 137.65, 136.27, 132.09, 131.07, 129.35, 128.85, 125.08, 124.98, 124.16, 123.99, 123.21, 116.33, 27.06. HRMS (FAB$^+$) [M= $C_{18}H_{15}NO_2$], calculated 277.1103, found 277.1103.

Synthesis of **JH-PN3**

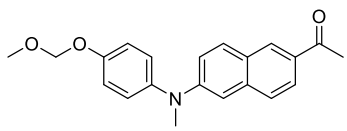

JH-PN3

JH-PN1 (406 mg, 1.263 mmol), methyl iodide (10 equiv.) and K_2CO_3 (3 equiv.) were stirred in acetone 20 ml at 60 ℃ for 2 days. The mixture was then concentrated in vacuo, diluted with CH_2Cl_2 and washed with water. The crude product was purified by silica gel column chromatography using Hexane/EtOAc (6:1) as eluent to give **JH-PN3** in 68% yield. ^{1}H NMR (300 MHz, $CDCl_3$): δ 8.34 (s, 1H), 7.95 (dd, J = 8.7, 1.62 Hz, 1H), 7.68 (dd, J = 18.3, 9.3 Hz, 2H), 7.22 – 7.04 (m, 6H), 5.21 (s, 2H), 3.55 (s, 3H), 3.41 (s, 3H) 2.69 (s, 3H); ^{13}C NMR (75.47 MHz, $CDCl_3$): δ 197.76, 154.88, 149.37, 142.18, 137.59, 131.34, 130.21, 130.15, 127.46, 126.41, 126.07, 124.66, 118.88, 117.55, 107.42, 94.70, 56.11, 40.75, 26.47. HRMS (FAB$^+$) [M= $C_{21}H_{21}NO_3$], calculated 335.1521, found 335.1521.

Synthesis of **JH-PN4**

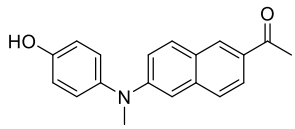

JH-PN4

To a solution of **JH-PN3** (335 mg, 1 mmol) in dry CH_2Cl_2 (5 ml), trifluoroacetic acid (5 ml) was added dropwise at 0 ℃. The resulting solution was stirred at room temperature until TLC indicated that all starting materials were consumed. The mixture was then concentrated in vacuo and azeotroped with toluene three times to give compound **JH-PN4**. The crude product was then purified by silica gel column chromatography using Hexane/EtOAc (4:1) as eluent to give **JH-PN4** in 99% yield. ^{1}H NMR (300 MHz, $CDCl_3$): δ 8.32 (s, 1H), 7.95 (dd, J = 10.3, 7 Hz, 1H), 7.67 (dd, J = 19.7, 10.6 Hz, 2H), 7.16 – 6.89 (m, 6H), 4.78 (s, 1H), 3.40 (s, 3H), 2.66 (s, 3H); ^{13}C NMR (75.47 MHz, DMSO-d_6): δ 198.15, 153.63, 149.613, 141.06, 137.67, 131.16, 130.33, 130.17, 127.97, 126.37, 125.91, 124.66, 118.64, 116.61, 106.98, 40.76, 26.44. HRMS (FAB^+) [M= $C_{19}H_{17}NO_2$], calculated 291.1259, found 291.1259.

Two-Photon Fluorescence Microscopy.

The two-photon fluorescence microscopy images were obtained with a DMI6000B Microscope (Leica) by exciting the probes with a mode-locked titanium-sapphire laser source (Mai Tai HP; Spectra Physics, 80 MHz pulse frequency, 100 fs pulse width)set at wavelength 740 nm and output power 2679 mW, which corresponded to approximately 1.5 mW average power in the focal plane.

Measurement of Two-Photon Cross Section.

The two-photon cross section (δ) was measured with femtosecond (fs) fluorescence measurement technique as described.[9] Rhodamine 6G was used as the reference. The intensities of the two-photon excited fluorescence spectra of the reference and sample were obtained at the same excitation wavelength. The TPA cross section was calculated by using $\delta = \delta_r(S_s\Phi_r\varphi_r c_r)/(S_r\Phi_s\varphi_s c_s)$: where the subscripts s and r stand for the sample and reference molecules. The intensity of the signal collected by a CCD detector was denoted as S. Φ is the fluorescence quantum yield. φ is the overall fluorescence collection efficiency of the experimental apparatus. The number density of the molecules in solution was denoted as c. δ_r is the TPA cross section of the reference molecule.

Cell Culture.

All cells were plated on glass-bottomed dishes (NEST) before imaging for two days. They were maintained in a humidified atmosphere of 5/95 (v/v) of CO_2/air at 37 ℃. The cells were incubated with **JH-PN4** at 37 ℃ under 5 % CO_2 for 30 min, washed three times with phosphate buffered saline (PBS; Gibco), and then imaged. The culture mediums for Raw 264.7 cells (ATCC, Manassas, VA, USA): DMEM (WelGene Inc, Seoul, Korea) supplemented with 10 % FBS (WelGene), penicillin (100 units/ml), and streptomycin (100 μg/mL).

B.1.5. Reference

[1] Jou, M. J.; Jou, S. B.; Guo, M. J.; Wu, H. Y.; Peng, T. I. *Ann. N. Y. Acad. Sci.* **2004**, *1011*, 45.

[2] Helmchen, F.; Denk, W. *Nat. Methods*, **2005**, *2*, 932–940.

[3] (a) Kim, H. M.; Cho, B. R. *Acc. Chem. Res.* **2009**, *42*, 863–872; (b) Yao, S.; Belfield, K. D. *Eur. J. Org. Chem.* **2012**, 3199–3217; (c) Liu, F.; Wu, T.; Cao, J.; Cui, S.; Yang, Z.; Qiang, X.; Sun, S.; Song, F.; Fan, J.; Wang, J. ; Peng, X.; *Chem. – Eur. J.* **2013**, *19*, 1548–1553; (d) Li, L.; Zhang, C. W.; Chen, G. Y.; Zhu, B.; Chai, C.; Xu, Q. H.; Tan, E. K.; Zhu, Q.; Lim, K. L.; Yao, S. Q. *Nat. Commun.* **2014**, *5*, 3276; (e) Dong, X.; Heo, C. H.; Chen, S.; Kim, H. M.; Liu, Z. *Anal. Chem.* **2014**, *86*, 308–311; (f) Zhou, L.; Zhang, X.; Wang, Q.; Lv, Y.; Mao, G.; Luo, A.; Wu, Y.; Wu, Y.; Zhang, J.; Tan, W. *J. Am. Chem. Soc.* **2014**, *136*, 9838–9841.

[4] (a) Lee, H.W.; Heo, C. H.; Sen, D.; Byun, H. O.; Kwak, I. H.; Yoon, G.; Kim, H. M. *Anal. Chem.* **2014**, *86*, 10001–10005; (b) Li, L.; Shen, X.; Xu, Q. H.; Yao, S. Q. *Angew. Chem., Int. Ed.* **2013**, *52*, 424–428; (c) Li, L.; Ge, J.; Wu, H.; Xu, Q. H.; Yao, S. Q. *J. Am. Chem. Soc.* **2012**, *134*, 12157–12167.

[5] (a) Li, X.; Tao, R.; Hong, L.; Cheng, J.; Jiang, Q.; Lu, Y.; Liao, M.; Ye, W.; Lu, N.; Han, F.; Hu, Y.; Hu, Y. *J. Am. Chem. Soc.* **2015**, *137*, 12296-12303; (b) Peng, T.; Wong, N.; Chen, X.; Chan, Y.; Ho, D.H.; Sun, Z.; Hu, J.J.; Shen, J.; El-Nezami, H.; Yang, D. *J. Am. Chem. Soc.* **2014**, *136*, 11728−11734

[6] (a) Kim, H. M.; Seo, M. S.; An, M. J.; Hong, J. H.; Tian, Y. S.; Choi, J. H.; Kwon, O.; Lee, K. J.; Cho, B. R. *Angew. Chem., Int. Ed.* **2008**, *47*, 5167.; (b) Rao, A. S.; Kim, D.; Nam, H.; Jo, H.; Kim, K. H.; Ban, C.; Ahn, K. H. *Chem. Commun.* **2012**, *48*, 3206.; (c) Rao, A. S.; Kim, D.; Wang, T.; Kim, K. H.; Hwang, S.; Ahn, K. H. *Org. Lett.* **2012**, *14*, 2598.; (d) Kim, H. M.; An, M. J.; Hong, J. H.; Jeong, B. H.; Kwon, O.; Hyon, J. Y.; Hong, S. C.; Lee, K. J.; Cho, B. R. *Angew. Chem., Int. Ed.* **2008**, *47*, 2231.

[7] Zhang, Q.; Zhang, N.; Long, Y.; Qian, X.; Yang, Y. *Bioconjugate Chem.* Article ASAP, DOI: 10.1021/acs.bioconjchem.5b00396

[8] Rejca, L.; Fabrisa, J.; Adrovića, A.; Kasuniča, M.; Petrič, A. *Tetrahedron Lett.* **2014**, *55*, 1218-1221

[9] Lee, S. K.; Yang, W. J.; Choi, J. J.; Kim, C. H.; Jeon, S. J.; Cho, B. R. *Org. Lett.* **2005**, *7*, 323.

B.2. Lanthanide-based Two-Photon Probes for Peroxynitrite

B.2.1. Introduction

Two-photon excitable lanthanide complexes have been developed and have shown the possibility of sensitization of the lanthanide with two-photon excitable sensitizer. [1,2,3,4,5] Some of the lanthanide complexes succeeded in penetrating the cells. [6,7,8] However, these probes are just for imaging the cell and not for detecting any specific target. Many groups have tried to develop a lanthanide-based two-photon probe that detects a specific target for biomedical application. Because it can offer advantages to both the two-photon probes and lanthanide-based probes. The advantages such as localized excitation, reduced photodamage, longer observation time, and greater tissue penetration depth, show sharp, line-like emission bands whose wavelengths are same with various environments and long excited state life time allowing time-resolved spectroscopy which can eliminate interferences that are caused by scattering and autofluorescence in biological conditions. However, this has not been developed. Therefore we designed and synthesized the lanthanide-based two-photon excitable complex for detecting peroxynitrite.

B.2.2. Results and Discussion

Design of Probes

We designed **Tb-PN** and **Eu-PN** with modification of **JH-PN4** in section B.1. **JH-PN4** was used as sensitizer of lanthanides and a targeting moiety. (Figure 1) When the N-phenyl group, the quencher, is dearylated by $ONOO^-$, the excited state of the sensitizer (acedan) can go through an intersystem crossing according to the heavy atom effect by lanthanide. Then, the energy transfer from the resulting triplet excited state to the lanthanide can occurs. Therefore, two-photon excited lanthanide phosphorescence can be detected.

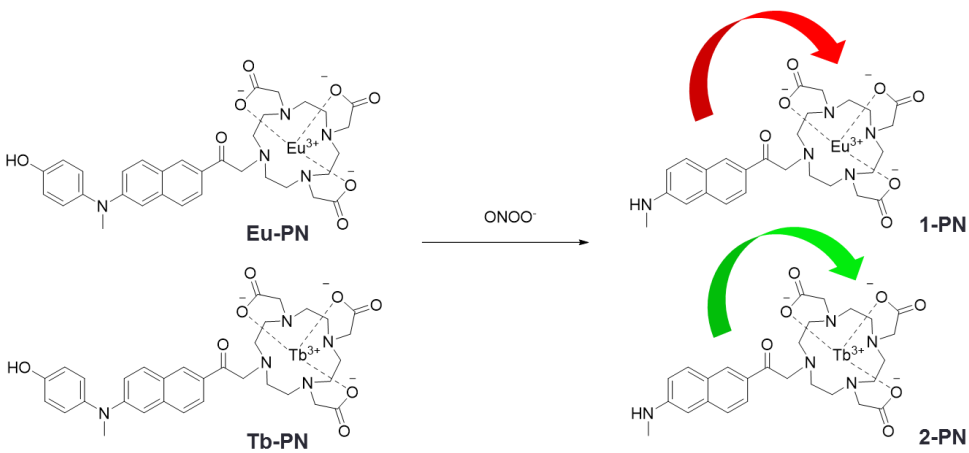

Figure 1. Design of probes

Luminescence responses of probes

We tested the luminescence responses of probes to $ONOO^-$ in order to confirm whether the sensitization from **JH-PN4** to lanthanide occurs. 2 equiv. of ONOO- was added to the probe in 10 mM PBS solution (0.4% DMF, pH 7.4). However, expected responses were not observed. **Tb-PN** showed no luminescence with or without $ONOO^-$. **Eu-PN** showed the only detectable turn-on response with 2 equiv. of $ONOO^-$. (Figure 2)

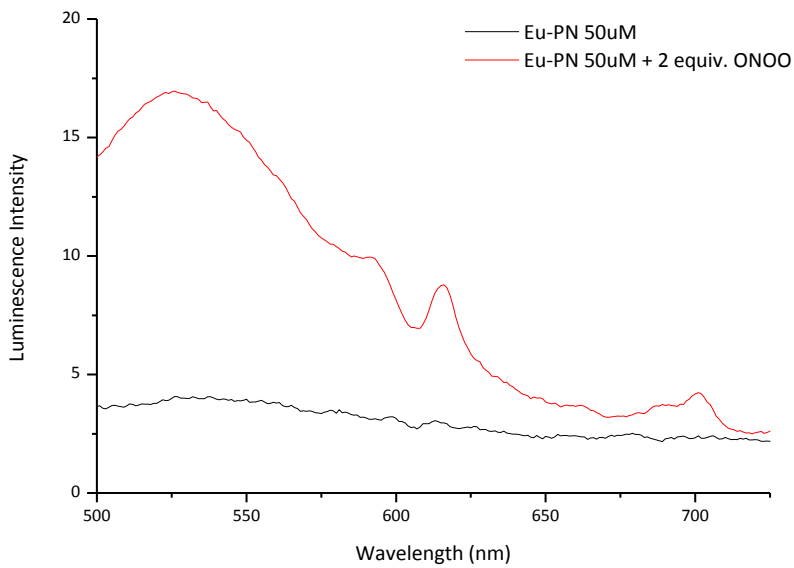

Figure 2. Luminescence spectra of **Eu-PN** (50 μM) with 2.0 equiv. of $ONOO^-$. Data were acquired at 25 ℃ in 10 mM phosphate buffer (0.4% DMF) at pH 7.4 with excitation at 400 nm. Reaction were carried out for 1h at room temperature before the fluorescence intensity of the probe solution was measured.

To explain these results, we observed phosphorescence of **Eu-PN** (50 μM) with 2.0 equiv. of $ONOO^-$. (Figure 3) Phosphorescence from the triplet excited state of sensitizer was a major part of the phosphorescence spectra and a minor phosphorescence of europium emission was observed. Through a maximum emission wave length of the sensitizer, we could calculate the energy level of triplet excited state of sensitizer (19230 cm^{-1}). Because the energy level of the triplet excited state (19230 cm^{-1}) is smaller than that of the emissive excited state of Tb^{3+} (20490 cm^{-1}). Thus, sensitization cannot occur resulting no luminescence of terbium. Otherwise, the energy level of the emissive excited state of Eu^{3+} was smaller than that of the sensitizer. The energy difference is greater than 1850 cm^{-1}, which means that sensitization is possible.[9]

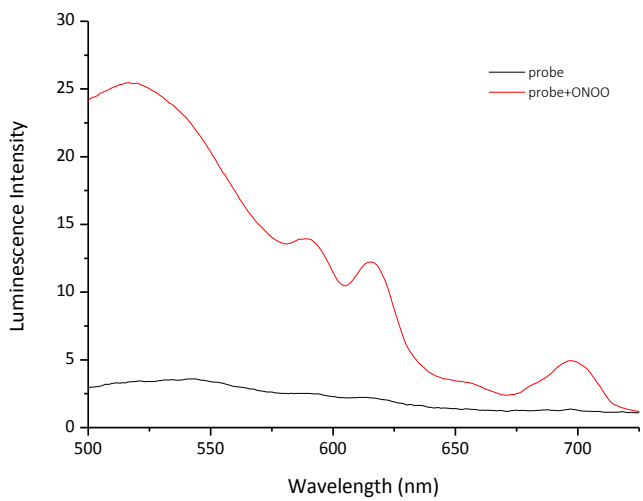

Figure 3. Phosphorescence spectra of **Eu-PN** (50 μM) with 2.0 equiv. of $ONOO^-$. Data were acquired at 25 ℃ in 10 mM phosphate buffer (0.4% DMF) at pH 7.4 with excitation at 400 nm, dealay time = 2 ms. Reaction were carried out for 1h at room temperature before the fluorescence intensity of the probe solution was measured.

However, the energy difference was so small (1990 cm^{-1}) that sensitization cannot occur efficiently. As a result, only a very weak emission of Eu^{3+} is observed. (Figure 2, 3)

B.2.3. Conclusion

We designed and synthesized the lanthanide-based two-photon probe detecting peroxynitrite. However, the energy level of the triplet excited state of the sensitizer was too low to sensitize the lanthanide. Therefore, the sensitizer should be changed to another sensitizer with higher energy level of the triplet excited state to develop lanthanide based two-photon probe. In addition, targeting moiety also should be changed because of low reactivity. Further studies for developing new probes for other targets using 6-(benzo[d]oxazol-2-yl)-2-(N, N-dimethylamino) naphthalene (BODAN)[10] as fluorophore is ongoing.

B.2.4. Experimental Section

Synthesis and characterization of probes

All the chemicals were purchased from commercial suppliers and used without further purification except anhydrous solvents. Reactions were monitored by thin layer chromatography with Merck silica gel 60 F254 on aluminum foil. Merck silica gel 60 was used as stationary phase for column chromatography. Celite® 545 was used for filtration. All the ^{1}H and ^{13}C NMR spectra were recorded on Bruker DRX 300 NMR spectrometer. Fluorescence emission spectra were recorded with a JASCO FP-

6500 spectrometer and the slit width was 3 or 10 nm for excitation and 3 or 5 nm for emission. HRMS data were obtained from Agilent 6890 Series, with FAB positive mode. Following figure is synthetic scheme for probes. (LiHMDS = lithium bis(trimethylsilyl)amide, THF = tetrahydrofuran, ACN = acetonitrile, TFA = trifluoroacetic acid, DCM = dichloromethane, MeOH = methanol.)

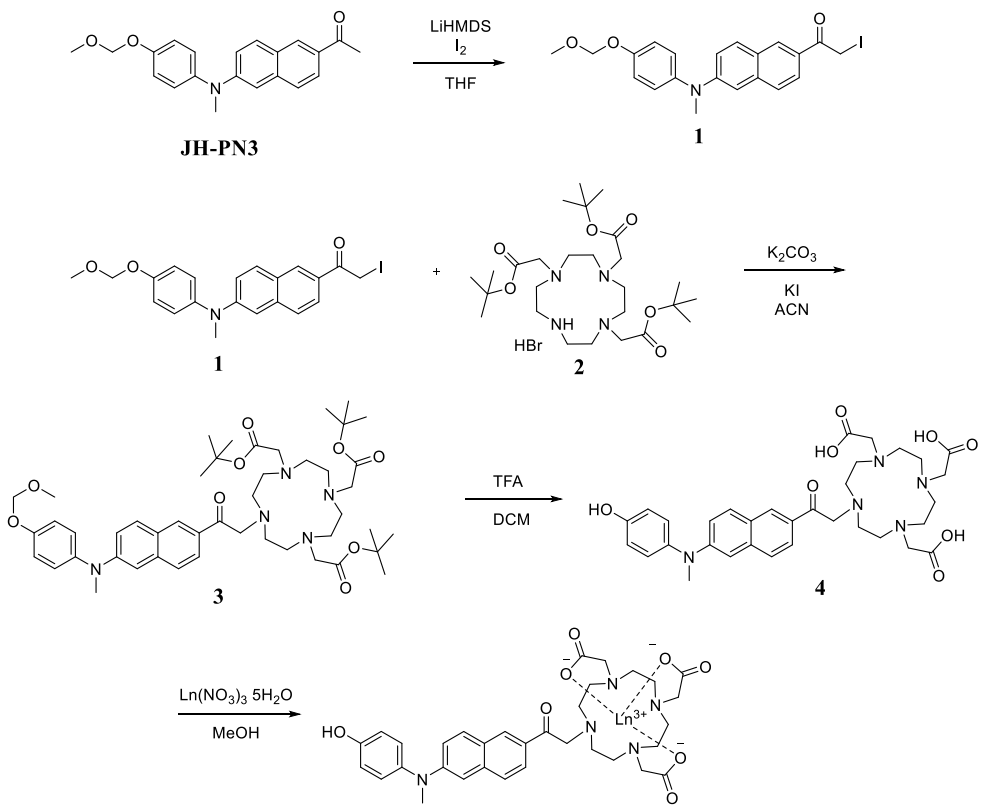

Ln = Eu (**Eu-PN**), Tb (**Tb-PN**)

Compound **JH-PN3** (see section B.1.4) and **3** [11] was prepared by the literature method and synthesis of the other compounds is described below.

Synthesis of **1**

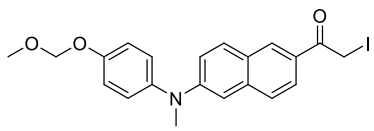

1

JH-PN3 (320 mg, 0.954 mmol) was dissolved in dry THF (5 ml) under N_2. LiHMDS (1.0 M in THF, 1.3 ml) was added dropwisely to **JH-PN3** solution at -78 °C in dark. After stirring 30 min, I_2 (242 mg, 0.954 mmol) in THF (5 ml) was added dropwisely over 5 min to solution. After stirring 30 min, the temperature was changed to 0 °C and the reaction was quenched with 1 M $NaHSO_4$ (2 ml), water (5 ml) and ether (30 ml). The mixture was washed twice with $Na_2S_2O_3$ and water and brine. And then, it was concentrated in vacuo and purified by silica gel column chromatography using Hex/EtOAc (6:1) as eluent to give **1** in 93% yield. ^{1}H NMR (300 MHz, $CDCl_3$): δ 8.37 (s, 1H), 7.94 (d, J = 8.57, 1H), 7.69 (dd, J = 19.97, 0 Hz, 2H), 7.21 – 7.03 (m, 6H), 5.23 (s, 2H), 4.46 (s, 2H), 3.55 (s, 3H), 3.42 (s, 3H); ^{13}C NMR (75.47 MHz, $CDCl_3$): δ 192.36, 155.06, 149.77, 141.92, 137.95, 131.01, 130.36, 127.62, 127.35, 126.70, 125.93, 125.16, 118.91, 117.59, 107.19, 94.69, 56.14, 42.16, 40.77, 2.13.

Synthesis of **3**

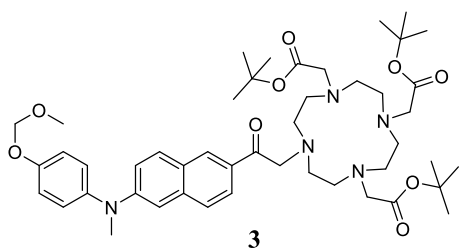

3

1 (400 mg, 0.867 mmol), **2** (0.9 equiv.) and K_2CO_3 (3 equiv.) is dissolved in Acetonitrile 10 ml and refluxed at 60 °C. After stirring overnight, the mixture was concentrated in vacuo. And then, it was worked up with CH_2Cl_2, MeOH and water. The crude product was purified by silica gel column chromatography using CH_2Cl_2/MeOH (100:1 to 20:1) as eluent to give **1** in 70% yield. ^{1}H NMR (300 MHz, $CDCl_3$): δ 8.27 (s, 1H), 7.81 (d, J = 8.66, 1H), 7.65 (dd, J = 24.81, 7.65 Hz, 2H), 7.19 – 6.99 (m, 6H), 5.20 (s, 2H), 4.08 (s, 2H), 3.53 (s, 3H), 3.40 (s, 3H), 3.40 – 2.10 (m, 22H), 1.49 – 1.27 (m, 27H) ; ^{13}C NMR (75.47 MHz, $CDCl_3$): δ 198.55, 172.76, 155.03, 149.55, 141.90, 137.87, 130.20, 129.65, 129.40, 127.60, 126.47, 125.80, 123.83, 118.77, 117.57, 107.00, 94.70, 81.99, 81.90, 77.29, 59.97, 56.11, 55.86, 55.66, 40.73, 27.34, 27.85.

Synthesis of **Ln-PN**

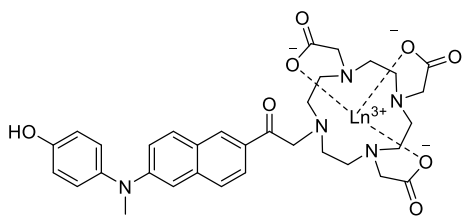

Ln = Eu (**Eu-PN**), Tb (**Tb-PN**)

3 (20 mg, 0.0236 mmol) was dissolved in CH_2Cl_2 (0.5 ml). CH_2Cl_2 (0.5 ml) and TFA (0.5 ml) was added dropwisely at 0 °C to make CH_2Cl_2/TFA (2:1) solution. After stirring overnight, the mixture was concentrated in vacuo. And then, the **4** was made in 98.6% yield. **4** is used without further purification; **4** and $Ln(NO_3)_3.5H_2O$ (1.2 equiv.) was dissolved in MeOH/H_2O (2:3) solution and refluxed for 2days at 60 °C. And then, acetone was poured to precipitate and the precipitation was filtered to be purified. The product **Ln-PN** is made in 54.8~60% yield.

Eu-PN in 54.8% yield. HRMS (FAB^+) [M= $C_{33}H_{38}EuN_5O_8$], calculated 786.2011, found 786.2014. UV−vis (H_2O) λ max (ε /M−1 cm−1): 260 nm (9048), 300 nm (3428), 421 nm (3944).

Tb-PN in 60% yield. HRMS (FAB^+) [M= $C_{33}H_{38}N_5O_8Tb$], calculated 792.2052, found 786.2052. UV−vis (H_2O) λ max (ε /M−1 cm−1): 256 nm (5218), 302 nm (2094), 394 nm (1912).

B.2.5. Reference

[1] Piszczek, G.; Maliwal, B. P.; Gryczynski, I.; Dattelbaum, J.; Lakowicz, J. R. *Journal of Fluorescence*, **2011**, *11*, 101-107

[2] Picot, A.; Malvolti, F.; Guennic, B. L.; Baldeck, P. L.; Gareth Williams, J. A.; Andraud, C.; Maury O. *Inorg. Chem.* **2007**, *46*, 2659-2665

[3] Hao, R.; Li, M.; Wang, Y.; Zhang, J.; Ma, Y.; Fu, L.; Wen, X.; Wu, Y.; Ai, X.; Zhang, S.; Wei, Y. *Adv. Funct. Mater.* **2007**, *17*, 3663–3669

[4] Fu, L.; Wen, X.; Ai, X.; Sun, Y.; Wu, Y.; Zhang, J.; Wang, Y. *Angew. Chem. Int. Ed*. **2005**, *44*, 747 –750

[5] D'Ale´o, A.; Picot, A.; Baldeck, P. L.; Andraud, C.; Maury, O. *Inorg. Chem.* **2008**, *47*, 10269-10279

[6] Picot, A.; D'Ale´o, A.; Baldeck, P. L.; Grichine, A.; Duperray, A.; Andraud, C.; Maury, O. *J. Am. Chem. Soc.* **2008**, *130*, 1532-1533.

[7] Eliseeva, S.V.; Aubo¨ck, G.; Mourik, F. V.; Cannizzo, A.; Song, B.; Deiters, E.; Chauvin, A.; Chergui, M.; Bu¨ nzli, J. G. *J. Phys. Chem. B*, **2010,** *114*, 2932–2937

[8] Lo, W.; Kwok, W.; Law, G.; Yeung, C.; Chan, C. T.; Yeung, H.; Kong, H.; Chen, C.; Murphy, M. B.; Wong, K.; Wong, W. *Inorg. Chem*. **2011**, *50*, 5309–5311

[9] Latva, M.; Takalo, H.; Mukkala, V.-M.; Matachescu, C.; Rodriguez-Ubis, J.C.; Kankare, J.; *J. Lumin*. **1997**, *75* ,149.

[10] Rathore, K.; Lim, C. S.; Lee, Y.; Cho, B. R. *Org. Biomol. Chem.* **2014**, *12*, 3406

[11] Prasuhn, D. E.; Yeh, R. M.; Obenaus, A.; Manchester, M.; Finn, M. G. *Chem. Commun*. **2007**, 1269 –1271.

국문 초록

이광자 분광법은 근적외선 영역의 광자 2 개를 여기원으로 이용하는 것으로 생의학 연구의 유용한 도구로 사용되어 왔다. 그러나 이광자 여기가 가능한 과산화 아질산염에 대한 프로브는 현재까지 극소수만이 개발되어왔다. 현재까지 개발된 프로브들은 다양한 생물학적 환경에서 이광자 분광법을 이용하여 과산화 아질산염을 감지할 수 있지만, 과산화 아질산염에 대한 탐구를 더 진행하기 위해서는 개선된 이광자 흡수성을 보이는 프로브가 개발되어야 한다.

우리는 탈아릴화 반응을 이용해서 다른 활성 산소 종, 활성 질소 종들 가운데서 선택적으로 과산화 아질산염만을 감지하는 새로운 프로브를 개발하였다. 개발된 프로브는 과산화 아질산염에 높은 선택성과 감도를 가지며, 이전에 발표된 프로브들보다 더 나은 이광자 흡수성을 가진다.

여기서 더 나아가 우리는 란탄족 원소의 인광이 가지는 독특한 특징들을 도입하기 위해 이광자 여기가 가능한 란탄족 원소 복합체를 합성하였다. 추가적인 개선을 통해 이 란탄족 원소 기반의 이광자 프로브들은 아직 명확하게 밝혀지지 않은, 생물계에 존재하는 과산화 아질산염의 효과들을 발견하는 것에 사용될 수 있다.

주요단어 : 과산화 아질산염, 이광자 분광법, 형광 프로브, 란탄족 원소 복합체

학번 : 2013-22923

이학석사학위논문

이광자 분광법을 이용한 과산화 아질산염에 대한 프로브

Probes for Peroxynitrite Using Two-Photon Microscopy

2016년 2월

서울대학교 대학원

화학부 유기화학전공

박 진 희

이광자 분광법을 이용한 과산화 아질산염에 대한 프로브

Probes for Peroxynitrite Using Two-Photon Microscopy

지도교수 홍 종 인

이 논문을 이학석사 학위논문으로 제출함

2016년 2월

서울대학교 대학원

화학부 유기화학전공

박 진 희

박 진 희의 이학석사 학위논문을 인준함

2015년 12월

위 원 장 **Soon Hyeok Hong** (인)

부위원장 홍 종 인 (인)

위 원 박 승 범 (인)

Probes for Peroxynitrite Using Two-Photon Microscopy

by

Jin-Hee Park

Supervisor: Prof. Jong-In Hong

A Thesis for the Master Degree
in Organic Chemistry

Department of Chemistry
Graduate School
Seoul National University

Probes for Peroxynitrite Using Two-Photon Microscopy

Abstract

Two-photon microscopy (TPM), utilizing two near-infrared (NIR) photons as the excitation source, has become a useful tool for biomedical research. However, only a few two-photon excitable probes for peroxynitrite have been developed that can detect peroxynitrite in various biological conditions using two-photon microscopy. However, two-photon peroxynitrite probe with an improved two-photon absorbing property is still required for further exploration.

Recently, it was reported that peroxynitrite can trigger oxidative N-dearylation reaction which can be used to induce fluorescence turn-on response. Thus, we have developed a new probe that can selectively detect peroxynitrite among other ROS/RNSs (Reactive oxygen/nitrogen species) utilizing dearylation reaction. The probe is highly selective and sensitive to peroxynitrite and has better two-photon excitation properties than any previous reported probes.

Further, we synthesized two-photon excitable lanthanide complexes to introduce unique properties of lanthanide phosphorescence- Sharp, line-like emission bands with the same fingerprint wavelengths and narrow peak widths, and long excited-state lifetimes in the ms~μs range. With further modification, these lanthanide based two-photon probes can be used to discover the effects of peroxynitrite in biological systems which are not clearly understood.

Keyword : Peroxynitrite, Two-Photon Microscopy, Fluorescence Probes, Lanthanide complexes

Student Number : 2013-22923

Contents

A. Background

A.1. Two-Photon Probes

Fluorescence imaging with small-molecule probes has become an important tool for studying living systems since they can detect targets rapidly with good selectivity and sensitivity, and can be easily loaded into cells. However, one-photon microscopy (OPM) utilizing one photon (OP) with short wavelength (350−550 nm) has several limitations for cell imaging and deep tissue imaging because the short wavelength of a photon can cause shallow penetration depth, autofluorescence and cell damage.[1]

Otherwise, two-photon microscopy (TPM), utilizing two near-infrared (NIR) photons (Figure 1) [2], has been used to image cells, tissues and animals. TPM has many advantages, such as localized excitation, reduced photodamage, longer observation time, and greater tissue penetration depth in comparison to OPM.[3,4,5,6] Therefore, various two-photon probes have been developed and their usability in bioimaging has been demonstrated.[7,8,9,10,11,12]

To show better properties of two-photon probes for biological target, probes should have a large two-photon absorption cross section (δ, in units of GM = 10^{-50} cm^4 s $photon^{-1}$ $molecule^{-1}$), which means the probability of a two-photon absorption (TPA) process. Probes with large δ values can be excited by lower laser power which can minimize photodamage. [1] Through many experiments, guidelines to design a probe with large δ values have been reported. The most important points of these guidelines is that enhancing the intramolecular charge transfer (ICT) produces an increase in the δ values

of the molecule. [13,14,15,16,17] Many two-photon probes are designed based on ICT enhancement. (Figure 2) [1]

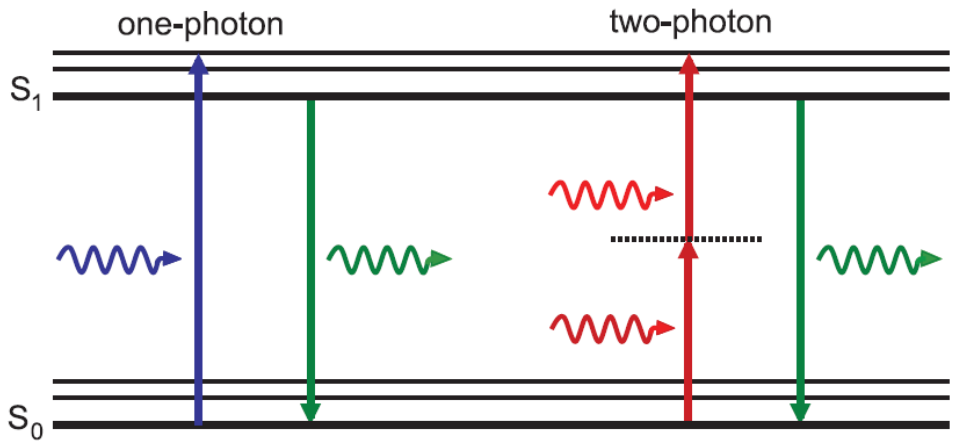

Figure 1. Concept of Two-photon excitation of fluorescence [2]

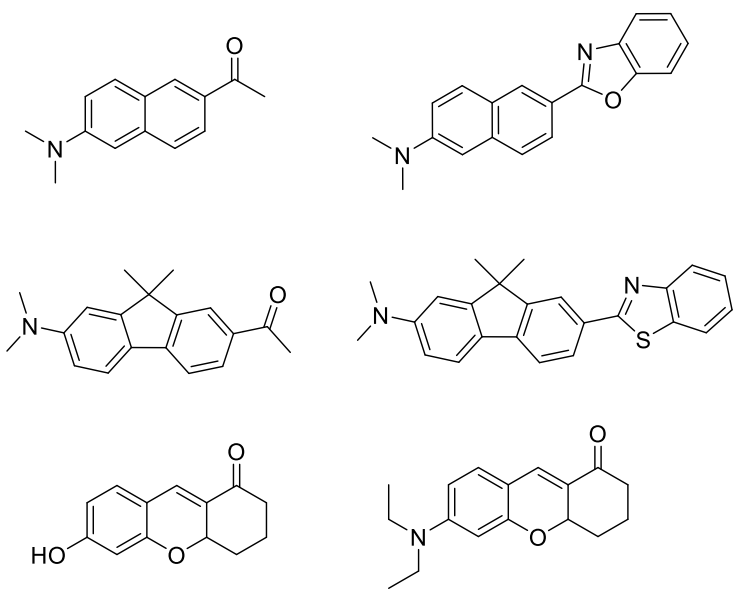

Figure 2. Representative two-photon fluorophores

A.2. Lanthanide-based Probes

Lanthanide based probes have been used widely in bioimaging because of the unique properties of lanthanide luminescence. The luminescence of lanthanides originates from the *f-f* electron transition in the *4f* subshell, which gives unique properties to the probe. First, the emissions of lanthanides are hardly affected by the surrounding environment and ligand field, since the 4f orbitals are shielded by 5s and 5p orbitals. Thus, lanthanide probes show sharp, line-like emission bands (the fingerprint wavelengths) whose wavelengths are constant regardless of the composing environments. Second, the luminescence has very long excited-state lifetime (ms to μs) because the *f-f* transitions are forbidden by the spin and Laporte rule.[18] This property allow lanthanide probes to image with time-resolved spectroscopy which can eliminate interferences caused by scattering and autofluorescence in biological conditions.

However, direct excitation of lanthanide complexes need very intense light sources because the *f-f* transition is forbidden. Thus, most lanthanide probes use a sensitizer (antenna), which can absorb the excitation light and sensitize the lanthanide ions (Figure 3). [19] When a sensitizer is excited by a light source, the singlet excited state of the sensitizer undergoes an intersystem crossing to the triplet excited state. Then, energy transfer occurs from the triplet excited state of the sensitizer to the emissive excited state of the lanthanide (sensitization). When sensitization occurs, the energy level of the triplet state of the sensitizer should be at least 1850 cm^{-1} higher than that of emissive excited state of the lanthanide.[20] If the energy gap is less than 1850 cm^{-1}, back energy transfer from the emissive excited state of the lanthanide to the triplet state of

the sensitizer can take place. This gives a long life time of the triplet excited state of the sensitizer, which can be quenched by O_2.

This O_2-effect can reduce the emission quantum yield. Therefore, the energy level of the triplet excited state of the sensitizer should be considered to design the lanthanide-based probe (Figure 4). [19] Reaction-based lanthanide probes induce the change of luminescence intensity by using a sensitizer whose structures are altered through the reaction with a target (Figure 5). [21]

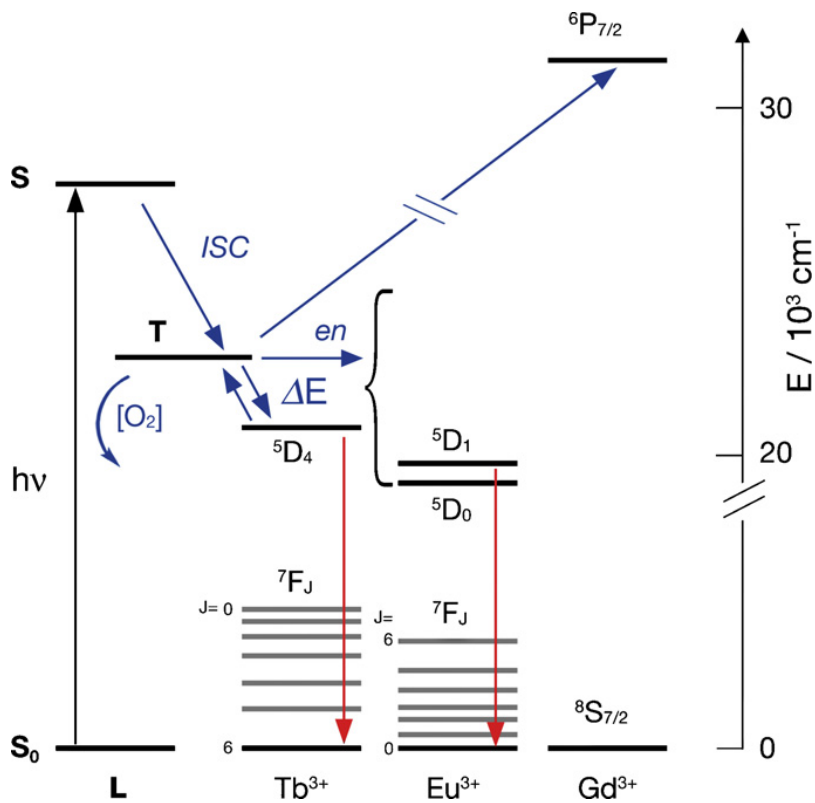

Figure 3. Sensitization of the luminescence in some lanthanide cations; blue arrows indicate non-radiative processes, red arrows indicate radiative processes.[19]

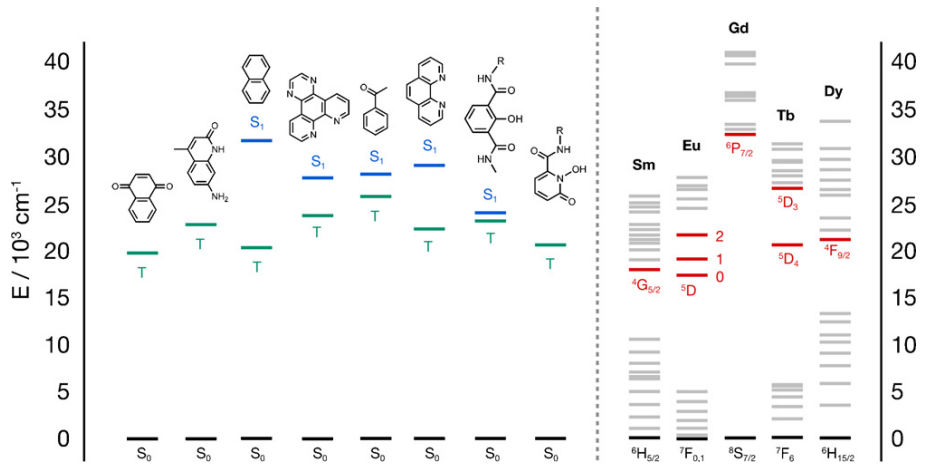

Figure 4. Energy diagram of the emissive levels of some lanthanide cations and sensitizers [19]

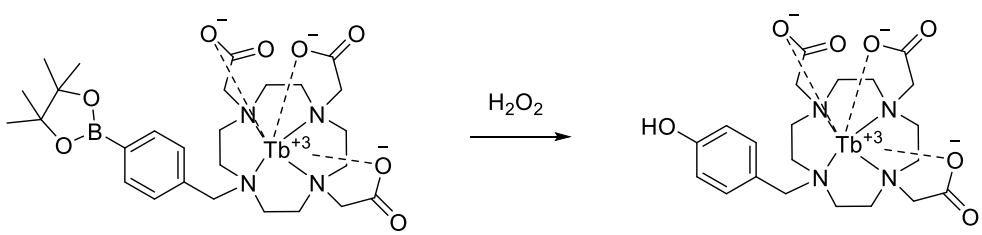

Figure 5. Lanthanide based hydrogen peroxide probe.

To develop efficient lanthanide based probes, coordinating ligand should be considered. Coordinating ligand should chelate lanthanide and protect the lanthanide ion from solvent coordination. Solvent coordination can cause vibrational energy transfer from the excited state of the lanthanide ion to the high-frequency X−H (X = C, N, O) oscillator, which shorten the lifetime of the excited state of the lanthanide (Figure 6). [22] Thus, chelating ligand should coordinate tightly with large coordination numbers in order to exclude as many vibrational oscillators from the lanthanide ion as possible.

Some lanthanide-based probes get turn-on responses from the change of the coordination number (Figure 7). [23] The lanthanide probe (Figure 7) shows increased emission intensity only when bicarbonate is coordinated to the lanthanide ion displacing the water molecules.

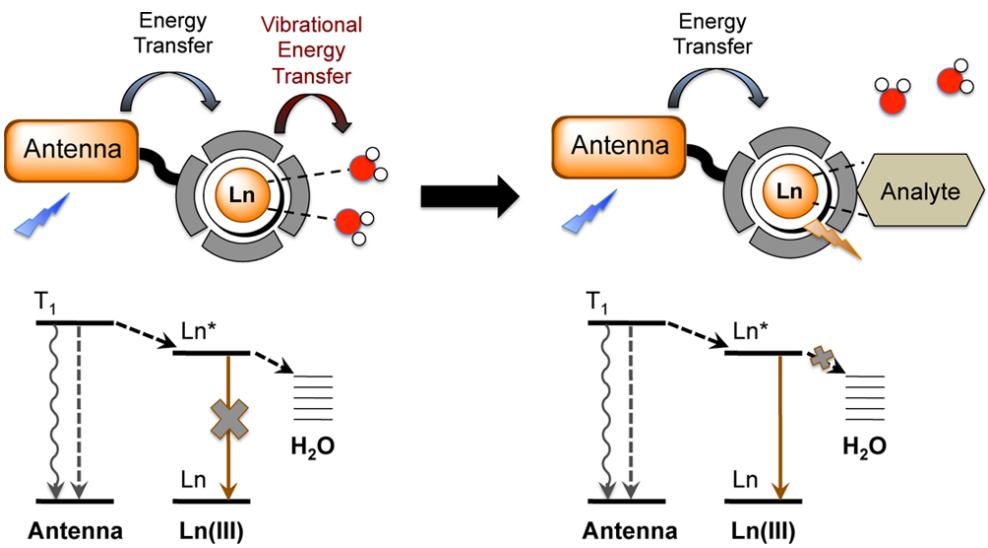

Figure 6. General scheme for the luminescence of lanthanide depending on the number of bound solvent (water) molecules. [22]

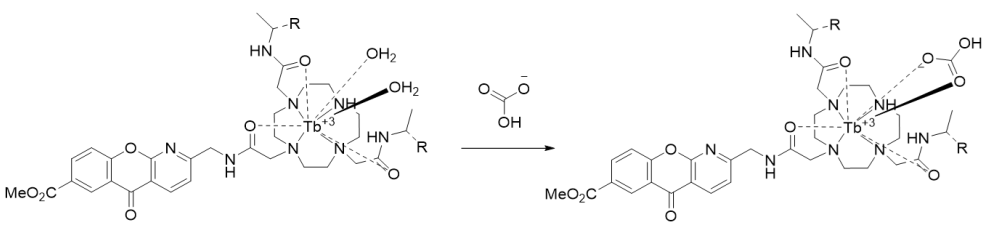

Figure 7. Bicarbonate-selective complexes that localize in the mitochondria

A.3. Luminescence probes for peroxynitrite

Peroxynitrite ($ONOO^-$) formed by the reaction between NO and $O_2^{\bullet-}$ is a strong oxidant found in biological system. $ONOO^-$ causes oxidation and nitration of biomolecules that are involved in a variety of physiological and pathological processes.[24] $ONOO^-$ plays important roles in immune responses against invading pathogens or cancer cells and redox regulation of signaling pathways.[25,26] However, $ONOO^-$ is also related to many diseases, such as cardiovascular, neurodegenerative, inflammatory and metabolic diseases, and pain, and cancer.[27]

However, the physiological roles of $ONOO^-$ are so far ambiguous due to its short half-life (<20 ms) and low concentration in the cells of living organisms. Therefore, development of new chemical tools for detecting peroxynitrite has been highly demanded.

Luminescence probes for peroxynitrite have been vigorously developed, and are able to detect $ONOO^-$ directly in cells. Most luminescence probes are designed as reaction-based probes whose targeting moieties are trifluorocarbonyl[28], phenyl boronic ester[29], hydrazine[30], selenium[31], nitrative aromatic ring[32] and electron-rich aromatic rings[33, 34].

A.4. References

[1] Kim, H. M.; Cho, B. R. *Chem. Rev.* **2015**, *115*, 5014−5055

[2] Benninger, R. K.; Piston, D. W. *Current Protocols in Cell Biology*. **2013**, *59*, 4.11.1–4.11.24.

[3] Helmchen, F.; Denk, W. *Nat. Methods*, **2005**, *2*, 932–940.

[4] (a) Kim, H. M.; Cho, B. R. *Acc. Chem. Res.* **2009**, *42*, 863–872; (b) Yao, S.; Belfield, K. D. *Eur.*

J. Org. Chem. **2012**, 3199–3217; (c) Liu, F.; Wu, T.; Cao, J.; Cui, S.; Yang, Z.; Qiang, X.; Sun, S.; Song, F.; Fan, J.; Wang, J. ; Peng, X.; *Chem. – Eur. J.* **2013**, *19*, 1548–1553; (d) Li, L.; Zhang, C. W.; Chen, G. Y.; Zhu, B.; Chai, C.; Xu, Q. H.; Tan, E. K.; Zhu, Q.; Lim, K. L.; Yao, S. Q. *Nat. Commun.* **2014**, *5*, 3276; (e) Dong, X.; Heo, C. H.; Chen, S.; Kim, H. M.; Liu, Z. *Anal. Chem.* **2014**, *86*, 308–311; (f) Zhou, L.; Zhang, X.; Wang, Q.; Lv, Y.; Mao, G.; Luo, A.; Wu, Y.; Wu, Y.; Zhang, J.; Tan, W. *J. Am. Chem. Soc.* **2014**, *136*, 9838–9841.

[5] (a) Bae, S. K.; Heo, C. H.; Choi, D. J.; Sen, D.; Joe, E. H.; Cho, B. R.; Kim, H. M. *J. Am. Chem. Soc.* **2013**, *135*, 9915–9923; (b) Kim, H. J.; Heo, C. H.; Kim, H. M. *J. Am. Chem. Soc.* **2013**, *135*, 17969–17977.

[6] (a) Lee, H.W.; Heo, C. H.; Sen, D.; Byun, H. O.; Kwak, I. H.; Yoon, G.; Kim, H. M. *Anal. Chem.* **2014**, *86*, 10001–10005; (b) Li, L.; Shen, X.; Xu, Q. H.; Yao, S. Q. *Angew. Chem., Int. Ed.* **2013**, *52*, 424–428; (c) Li, L.; Ge, J.; Wu, H.; Xu, Q. H.; Yao, S. Q. *J. Am. Chem. Soc.* **2012**, *134*, 12157–12167.

[7] Kim, H. M.; Cho, B. R. *Acc. Chem. Res.* **2009**, *42*, 863.

[8] Kim, H. M.; Cho, B. R. *Chem.-Asian J.* **2011**, *6*, 58.

[9] Sumalekshmy, S.; Fahrni, C. J. *Chem. Mater.* **2011**, *23*, 483.

[10] Yao, S.; Belfield, K. D. *Eur. J. Org. Chem.* **2012**, 3199.

[11] Kim, H. M.; Cho, B. R. *Oxid. Med. Cell. Longevity* **2013**, *2013*, 1−11.

[12] Kim, D.; Ryu, H. G.; Ahn, K. H. *Org. Biomol. Chem.* **2014**, *12*, 4550.

[13] Rumi, M.; Barlow, B.; Wang, J.; Perry, J. W.; Marder, S. R. *Adv. Polym. Sci.* **2008**, *213*, 1−95.

[14] Strehmel, B.; Strehmel, V. *Adv. Photochem*. **2007**, *27*, 111−354.

[15] Pawlicki, M.; Collins, H. A.; Denning, R. G.; Anderson, H. L. *Angew. Chem., Int. Ed.* **2009**, *48*, 3244.

[16] Belfield, K. D.; Yao, S.; Bonder, M. V. *Adv. Polym. Sci*. **2008**, *213*, 1−95.

[17] He, G. S.; Tan, L. S.; Zheng, Q.; Prasad, P. N. *Chem. Rev*. **2008**, *108*, 1245.

[18] Bünzli, J.-C. G.; Chauvin, A.-S.; Kim, H. K.; Deiters, E.; Eliseeva, S.V. *Coord. Chem. Rev*. **2010**, *254*, 2623.

[19] Armelaoa, L.; Quicib, S.; Barigelletti, F.; Accorsic, G.; Bottarod, G.; Cavazzinib, M.; Tondelloe, E. *Coord. Chem. Rev*. **2010**, *254*, 487

[20] Latva, M.; Takalo, H.; Mukkala, V.-M.; Matachescu, C.; Rodriguez-Ubis, J.C.; Kankare, J.; *J. Lumin*. **1997**, *75*,149.

[21] (a) Terai, T.; Kikuchi, K.; Iwasawa, S.-Y.; Kawabe, T.; Hirata, Y.; Urano, Y.; Nagano, T. *J. Am.*

Chem. Soc. **2006**, *128*, 6938; (b) Pershagen, E.; Nordholm, J.; Borbas, K. E. *J. Am. Chem. Soc.* **2012**, *134*, 9832; (c) Lippert, A. R.; Gschneidtner, T.; Chang, C. J. *Chem. Commun.* **2010**, *46*, 7510.

[22] Heffern, M. C.; Matosziuk, L. M.; Meade, T. J. *Chem. Rev.* **2014**, *114* , 4496–4539

[23] (a) Smith, D. G.; McMahon, B. K.; Pal, R.; Parker, D. *Chem. Commun.* **2012**, *48*, 8520; (b) McMahon, B. K.; Pal, R.; Parker, D. *Chem. Commun.* **2013**, *49*, 5363; (c) Smith, D. G.; Pal, R.; Parker, D. *Chem.-Eur. J.* **2012**, *18*, 11604.

[24] Koppenol, W. H.; Moreno, J. J.; Pryor, W. A.; Ischiropoulos, H.; Beckman, J. S. *Chem. Res. Toxicol.* **1992**, *5*, 834−842.

[25] (a) Radi, R. *J. Biol. Chem*. **2013**, *288*, 26464. (b) Liaudet, L.; Vassalli, G.; Pacher, P. *Front Biosci*. **2009**, *14*, 4809.

[26] (a) MacMicking, J.; Xie, Q. W.; Nathan, C. *Annu. Rev. Immunol.* **1997**, *15*, 323−350; (b) Bogdan, C. *Nat. Immunol*. **2001**, *2*, 907−916; (c) Chakravortty, D.; Hensel, M. *Microbes Infect.* **2003**, *5*, 621−627.

[27] (a) Pacher, P.; Beckman, J. S.; Liaudet, L. *Physiol. Rev.* **2007**, *87*, 315. (b) Szabo, C.; Ischiropoulos, H.; Radi, R. *Nat. Rev. Drug Discovery*, **2007**, *6*, 662. (c) Ferrer-Sueta, G.; Radi, R. *ACS Chem. Biol.* **2009**, *4*, 161.

[28] Peng, T.; Yang, D. *Org. Lett.* **2010**, *12*, 4932−4935.

[29] Chen, Z.-J.; Ren, W.; Wright, Q. E.; Ai, H.-W. *J. Am. Chem. Soc.* **2013**, *135*, 14940−14943

[30] Ambikapathi, G.; Kempahanumakkagari, S. K.; Lamani, B. R.; Shivanna, D. K.; Maregowda, H. B.; Gupta, A.; Malingappa, P. *J. Fluoresc*. **2013**, *23*, 705−712.

[31] Yu, F.; Li, G.; Zhao, G.; Chu, T.; Han, K. *J. Am. Chem. Soc.* **2011**, *133*, 11030−11033

[32] Ueno, T.; Urano, Y.; Kojima, H.; Nagano, T. *J. Am. Chem. Soc.* **2006**, *128*, 10640−1064

[33] Peng, T.; Wong, N.; Chen, X.; Chan, Y.; Ho, D.H.; Sun, Z.; Hu, J.J.; Shen, J.; El-Nezami, H.; Yang, D. *J. Am. Chem. Soc.* **2014**, *136*, 11728−11734

[34] Zhang, Q.; Zhang, N.; Long, Y.; Qian, X.; Yang, Y. *Bioconjugate Chem.* Article ASAP, DOI: 10.1021/acs.bioconjchem.5b00396

B. Two-Photon Probes for Peroxynitrite

B.1.Two-Photon turn-on probe for peroxynitrite

B.1.1. Introduction

Different types of luminescence probes have been developed to detect intracellular peroxynitrite directly. However, these probes are excited by photons with short wavelengths (from UV to visible light), thus limiting their use in cells and tissues due to autofluorescence, artificial reactive oxygen species (ROS) generation, and shallow penetration. [1]

Two-photon microscopy (TPM) utilizes two photons with a long wavelength (near infrared) for excitation. TPM has been used for biomedical research. TPM has many advantages such as localized excitation, low photodamage, and deep penetration depth. [2, 3, 4] Nonetheless, only a few two-photon excitable probes for $ONOO^-$ were reported.[5] These types of probes detected peroxynitrite in live cells and tissues using two-photon microscopy. However, a two-photon peroxynitrite probe with an advanced two-photon absorbing property is highly required for further investigation of $ONOO^-$.

In this thesis, we report a noble peroxynitrite probe (**JH-PN4**) that shows good selectivity among other ROS/RNSs (Reactive oxygen/nitrogen species) by utilizing a peroxynitrite-triggerd dearylation reaction.[5b] **JH-PN4** can also detect $ONOO^-$ in nanomolar concentration levels and have better two-photon excitation properties than previous reported probe. [5a]

B.1.2. Results and Discussion

Design of Probes

The **JH-PN4** is composed of 2-methylamino-6-acetylnaphthalene (acedan), a well-known two-photon fluorophore, as a reporting group [6] and N-methyl-*p*-hydroxyaniline as a targeting moiety. The N-phenyl group quenching the fluorescence of 2-methylamino-6-acetylnaphthalene can be eliminate efficiently by $ONOO^-$ with good selectivity among other ROS/RNSs. [5b] Dearylation can make the fluorescence of acedan recovered through making the probe have "push-pull" structure (Scheme 1A). In addition, we also synthesized probes **JH-PN1~JH-PN3** in order to investigate the N-, O- substituents effects. (Scheme 1B).

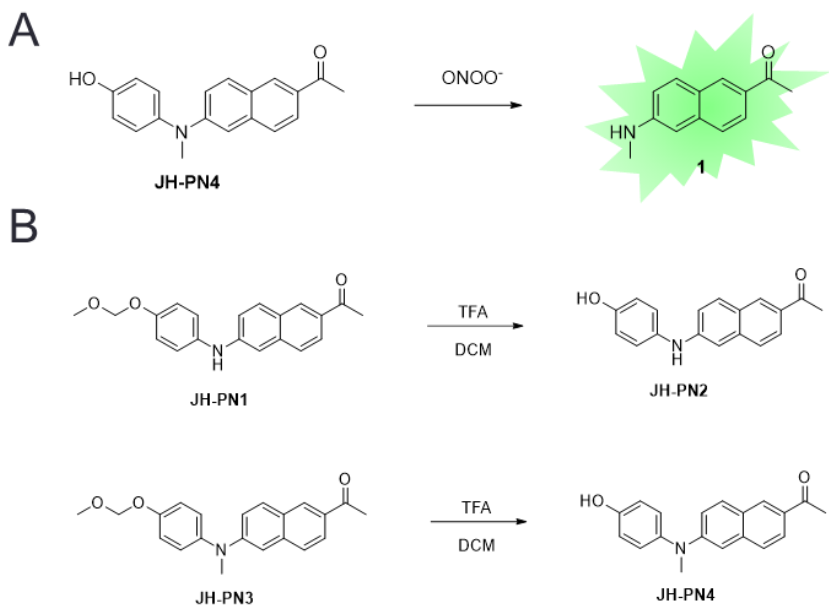

Scheme 1. (A) Sensing mechanism and (B) structures of **JH-PN1~4**. TFA = trifluoroacetic acid, DCM = dichloromethane.

Selectivity tests of JH-PN1~4

With **JH-PN1~4**, we performed a selectivity test for $ONOO^-$ among other ROS/RNSs in 10 mM phosphate-buffered saline (PBS) solution (0.4% DMF, pH 7.4). As expected, **JH-PN1, JH-PN3**, having a methoxymethyl ether group did not give any remarkable response to the $ONOO^-$ and other ROS species (Figures 1A and 1C). Also, **JH-PN2** composed of the diarylamino (Ar-NH-Ar′) group, show only slight increase in

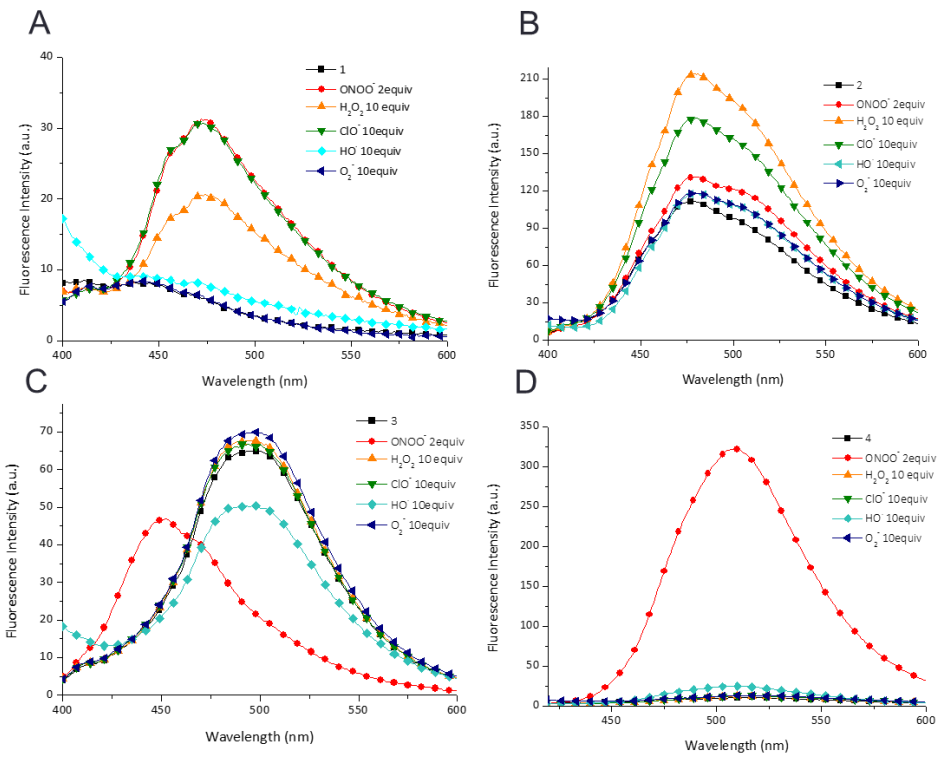

Figure 1. Fluorescence spectra of (A) **JH-PN1** (B) **JH-PN2** (C) **JH-PN3** (D) **JH-PN4** (20 μM) with various ROS/RNSs. (2.0 equiv. for $ONOO^-$, 10 equiv. for other ROSs). Data were acquired at 25 ℃ in 10 mM phosphate buffer with 0.4% dimethyl formamide (DMF) at pH 7.4 with excitation at 360 nm. Reaction were carried out for 1h at room temperature before the fluorescence intensity of the probe solutions was measured.

the fluorescence intensity upon the addition of $ONOO^-$ or other species (Figure 1B). This is probably due to the oxidation of diarylamine by the $ONOO^-$.[7]

Otherwise, the fluorescence intensity of **JH-PN4** at 509 nm was increased more than 32-fold when 2 equiv. of $ONOO^-$ were added. Moreover, any significant change was not observed with other excess ROS/RNSs (Figure 2). Although a slight increase of fluorescence intensity was observed with nitric oxide (NO), it is negligible because the amount of NO added to the probe was too large (2 mM) which cannot exist in the cells. In addition, fluorescence change with NO is much smaller than that with $ONOO^-$. Therefore, **JH-PN4** was chosen for the next experiments.

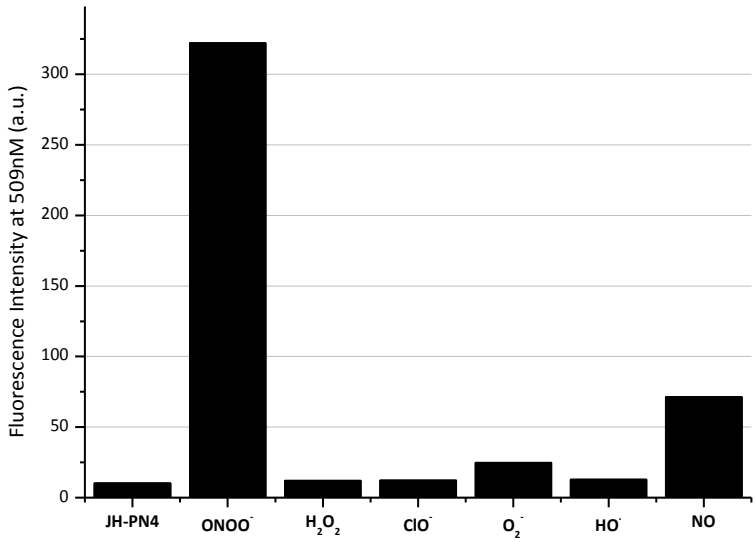

Figure 2. Fluorescence Intensity (λ_{em} = 509 nm) of **JH-PN4** (20 μM) with various reactive oxygen/nitrogen species [ROS/RNSs, 2.0 equiv. for $ONOO^-$, 10 equiv. for other ROSs, and 100 equiv. for nitric oxide (NO)]. Data were acquired at 25 ℃ in 10 mM phosphate buffer with 0.4% dimethyl formamide (DMF) at pH 7.4 with excitation at 360 nm. Reactions were carried out for 1h at room temperature before the fluorescence intensity of the probe solutions was measured.

Fluorescence response of JH-PN4

First, to test the sensitivity of **JH-PN4**, fluorescence change was measured with increasing concentrations of $ONOO^-$ (Figure 3). The fluorescence intensity of **JH-PN4** at 509 nm increased more than 57-fold with the addition of 5 equiv. of $ONOO^-$ (Figure 3A). This is due to the removal of the N-phenyl group, which quenches the

fluorescence of the probe, by dearylation. The detection limit of **JH-PN4** was estimated to be as low as 359 nM (Figure 3B, and 4), confirming a high sensitivity of **JH-PN4** to $ONOO^-$. However, the fluorescence intensity decreased with more than 5 equiv. of $ONOO^-$. These results probably arose from further oxidation of acedan produced by dearylation of **JH-PN4** with $ONOO^-$. The secondary amine group of acedan can be oxidized with excess $ONOO^-$, reducing the fluorescence of acedan. [5b, 7]

Then, we investigated the time-dependent fluorescence change of **JH-PN4** with 1 equiv. of $ONOO^-$ (Figure 5). **JH-PN4** showed a rapid turn-on response to $ONOO^-$ within 3s and the reaction was saturated within 10min (Figure 5B) proving that **JH-PN4** can rapidly detect $ONOO^-$ whose life time in intracellular condition is very short.

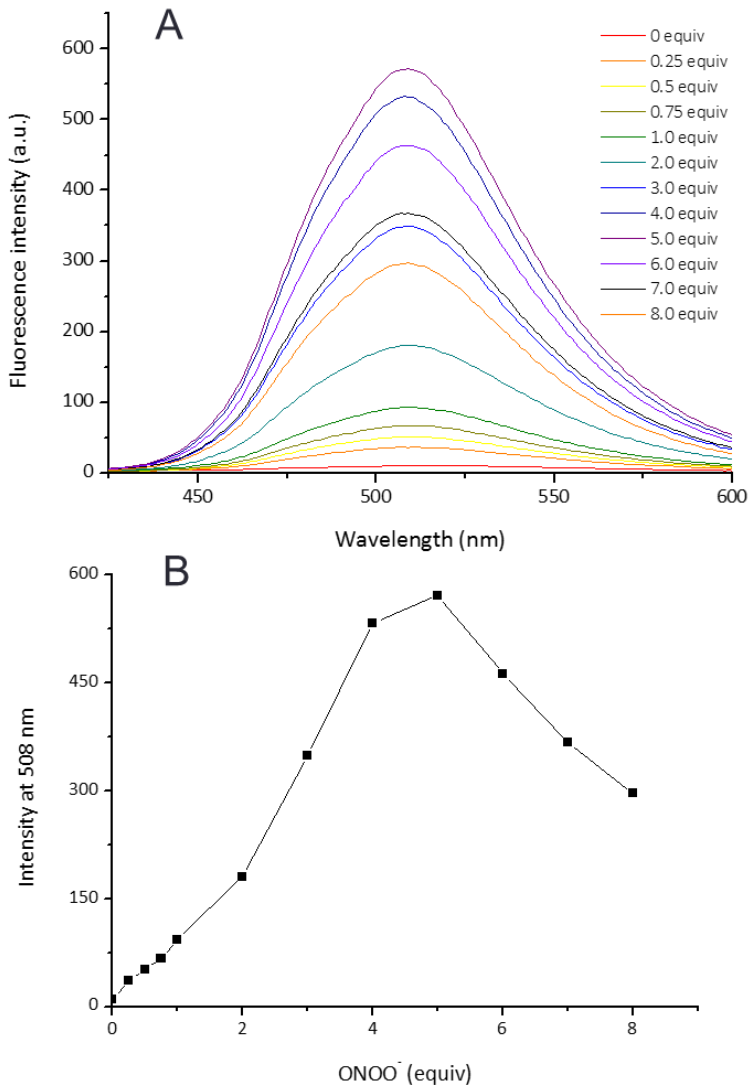

Figure 3. Testing the sensitivity of **JH-PN4**: (A) fluorescence spectra and (B) fluorescence intensity at 508 nm of **JH-PN4** (20 μM) with $ONOO^-$ (0~8 equiv.). Data were acquired at 25 ℃ in 10 mM phosphate buffer with 0.4% dimethyl formamide (DMF) at pH 7.4 with excitation at 360 nm. Reactions were carried out for 30 min at room temperature before the fluorescence intensity of the probe solutions was measured.

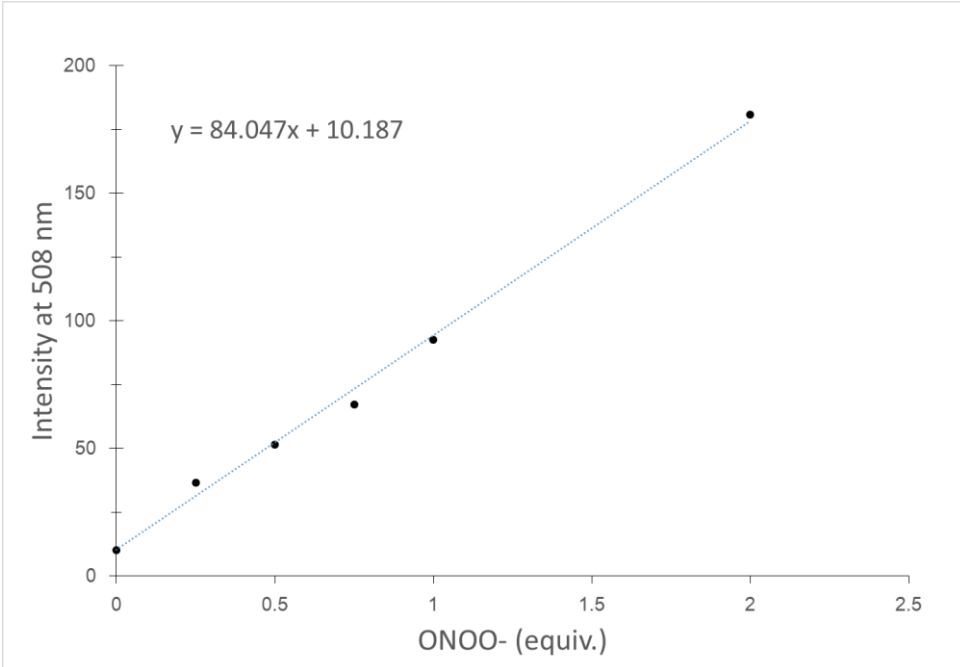

Figure 4. Linear plot of the fluorescence intensity at 508 nm of **JH-PN4** (20 μM) against a $ONOO^-$ concentration. Data were acquired at 25 ℃ in 10 mM phosphate buffer with 0.4% dimethyl formamide (DMF) at pH 7.4 with excitation at 360 nm. Reactions were carried out for 30 min at room temperature before the fluorescence intensity of the probe solutions was measured.

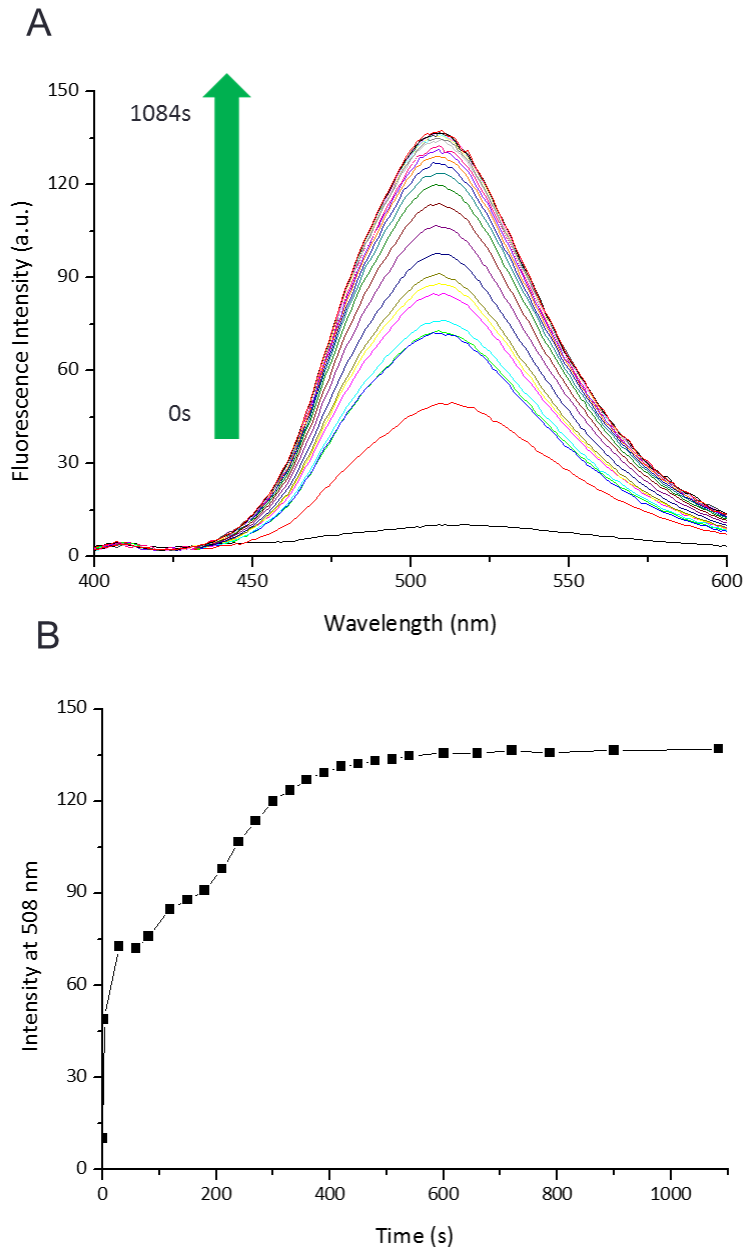

Figure 5. (A) Time-dependent fluorescence change and (B) time course of fluorescence Intensity (λem = 509 nm) of **JH-PN4** (10 μM) in 10 mM phosphate buffer saline (PBS) (0.2% DMF, pH 7.4) in the presence of 1.0 equiv. $ONOO^-$ (λ_{ex} = 360 nm).

Next, we measured the fluorescence change of **JH-PN4** with $ONOO^-$ using two-photon excitation mode (Figure 6). As expected, **JH-PN4** showed fluorescence turn-on response to $ONOO^-$ with two-photon excitation (Figure 6A). A maximum two-photon absorption cross section (σ_{max}) of **JH-PN4** with 3 equiv. of $ONOO^-$ was 8.8 GM at 740 nm which is an improved value when compared with previous reported probes.[5a] In addition, the value of a two-photon action cross section increased about 4 times with 3 equiv. of $ONOO^-$ (Figure 6B).

Effect of pH to Fluorescence of Probe 4

To test the availability of **JH-PN4** as a $ONOO^-$ probe, the fluorescence intensities of **JH-PN4** and product **1** was observed in a PBS with different pH values ranging from 4 to 9 (Figure 7). A noticeable change was not observed in various pH conditions. The fluorescence intensity of **JH-PN4** at 509 nm slightly increased in basic conditions (> pH 9), but was insignificant when compared to the change of fluorescence intensity with the addition of $ONOO^-$. Moreover, the fluorescence intensity of product **1** reduced at pH 4, which is also trivial. This suggests that **JH-PN4** is very stable in a range of pH conditions and is usable in a physiological condition.

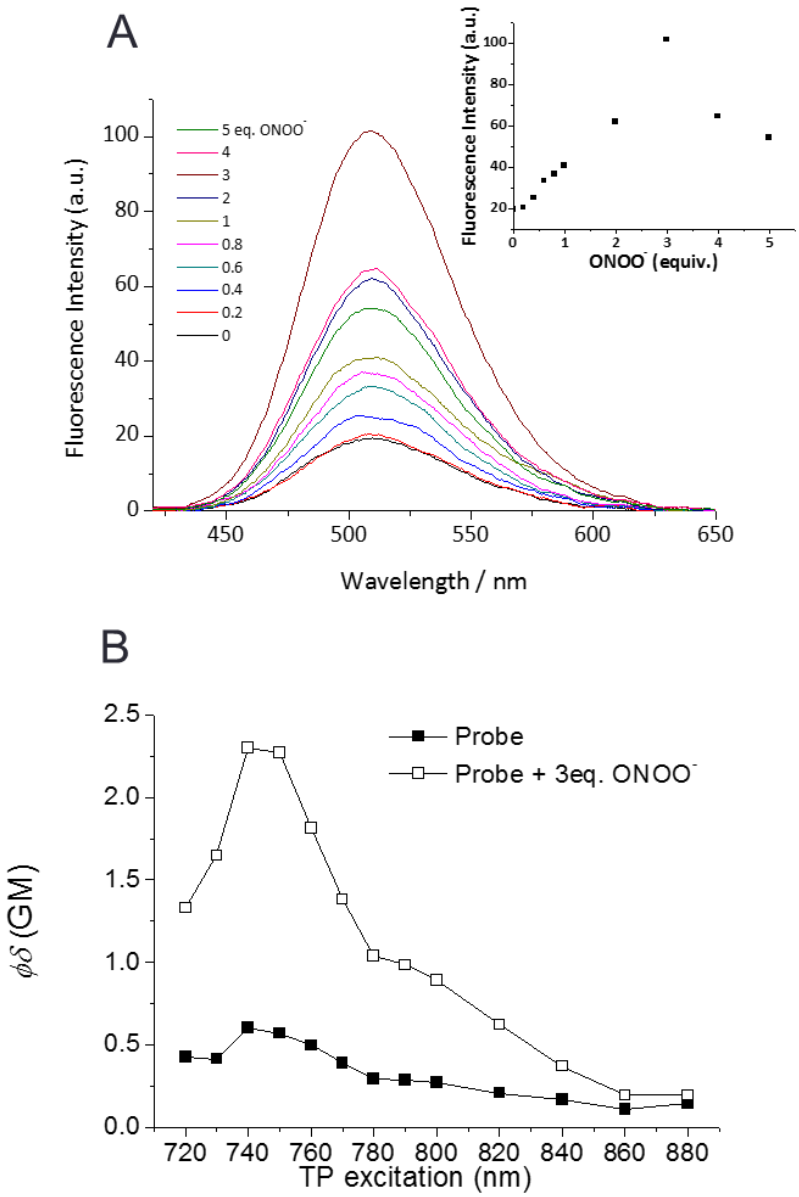

Figure 6. (A) Two-photon fluorescence spectra of **JH-PN4** (10 μM) with $ONOO^-$. Inset shows Two-photon fluorescence titration curve for **JH-PN4** with $ONOO^-$. The excitation wavelength was 740 nm. (B) Two-photon action spectra of **JH-PN4** in the absence (■) and in the presence of $ONOO^-$ (□). These data were measured in 10 mM phosphate buffer saline (PBS).

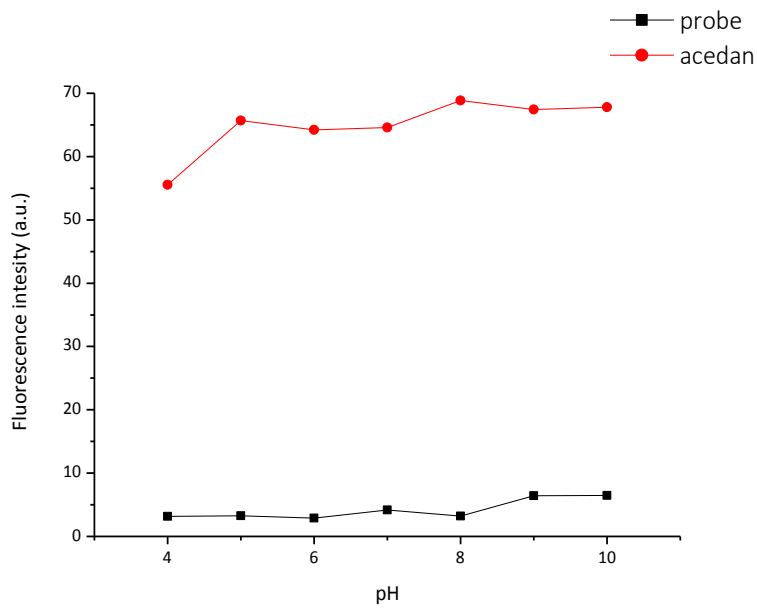

Figure 7. Fluorescence intensities at 509 nm of **JH-PN4** and **1** (10 μM) at various pH values. (λ_{ex} = 360 nm)

Live cell imaging

We tested the ability of **JH-PN4** to image $ONOO^-$ in live cells by two-photon microscopy. With SIN-1 (3-morpholinosydnonimine hydrochloride), exogenous $ONOO^-$ donor, (Figure 8) and endogenous $ONOO^-$, (Figure 9) intracellular fluorescence increased slightly. However, they were too small to overcome error range. (Figure 8B and 9B) It can be assumed that dearylation of the N-phenyl group in **JH-PN4** does not vigorously occurred compared with other probes.[5] The fact that the maximum fluorescence intensity of **JH-PN4** with $ONOO^-$ in fluorescence titration (Figure 3) is

much smaller than the estimated fluorescence intensity of product **1** support this assumption.

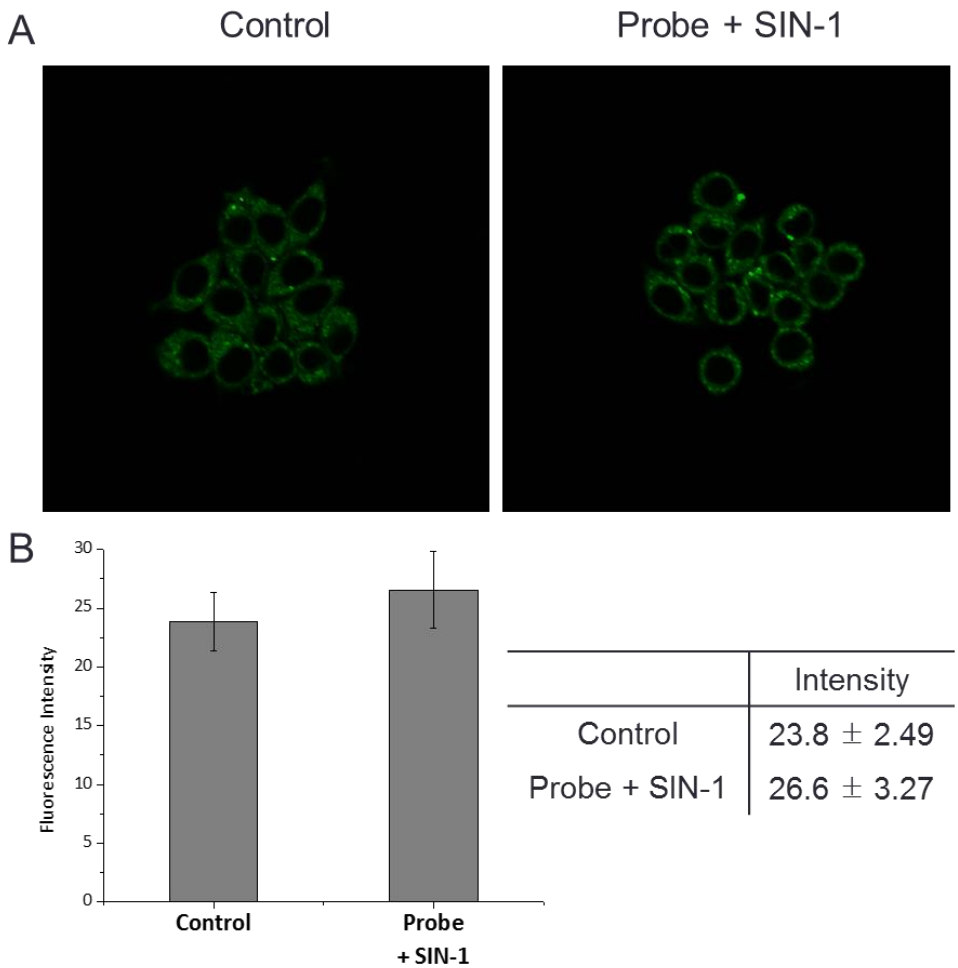

Figure 8. (A) Two-photon microscopy images of exogenous $ONOO^-$ donor with **JH-PN4** in RAW 264.7 macrophages. (B) Quantification of the fluorescence signals from (A). Cells were pre-treated with SIN-1 (10 μM) for 10 min, and then incubated with **JH-PN4** (10 μM) for 30 min. The intensities were collected at 400-600 nm upon excitation at 740 nm.

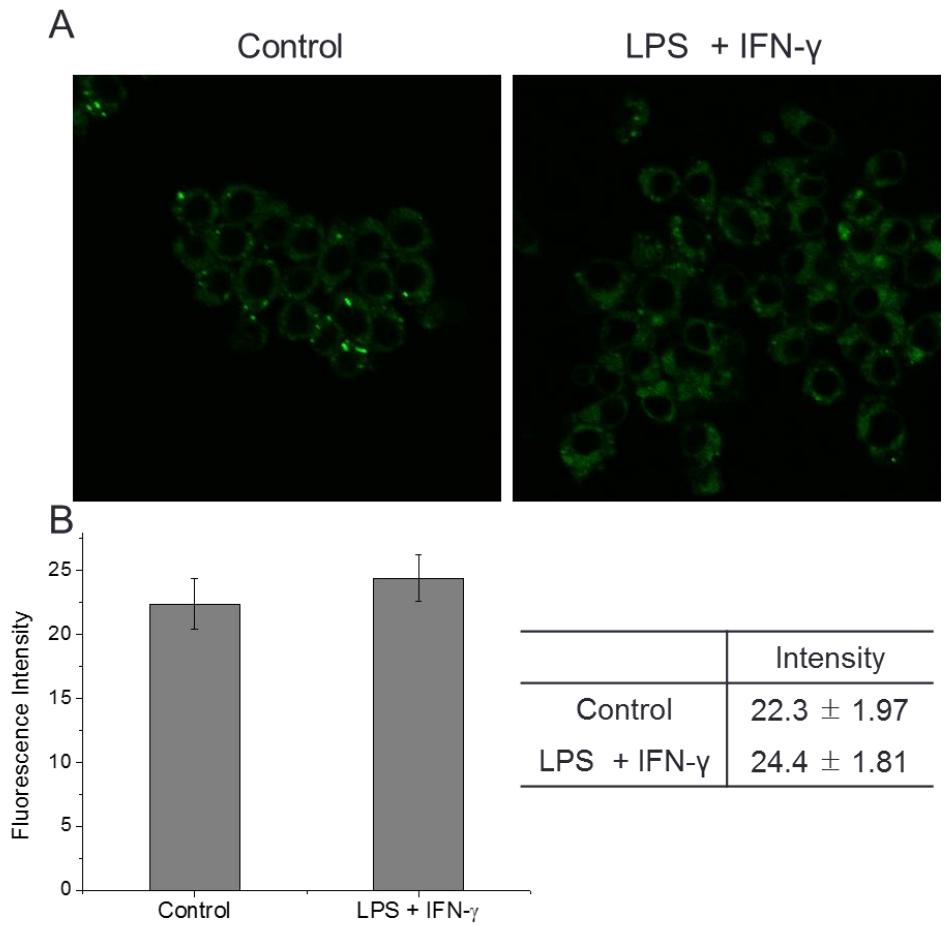

Figure 9. Two-photon microscopy images of endogenous $ONOO^-$ with **JH-PN4** in RAW 264.7 macrophages. Cells were pre-treated with LPS (1 μg/ml) and IFN-γ (100 ng/ml) for 14 h, and then incubated with **JH-PN4** (10 μM) for 30 min. The intensities were collected at 400-600 nm upon excitation at 740 nm.

B.1.3. Conclusion

We developed a two-photon turn-on probe for peroxynitrite using peroxynitrite-triggered dearylation. **JH-PN4** is a highly sensitive and selective probe for peroxynitrite among other ROS/RNSs and has improved two-photon excitation properties in comparison with previous reported probes. Thus, we imaged intracellular peroxynitrite with **JH-PN4,** but fluorescence increase was too small in cellular conditions. In the future research, further modification to increase the reactivity of targeting moiety should be conducted to develop useful tools for imaging cellular peroxynitrite.

B.1.4. Experimental Section

Synthesis and characterization of probes

All the chemicals were purchased from commercial suppliers and used without further purification except anhydrous solvents. Reactions were monitored by thin layer chromatography with Merck silica gel 60 F254 on aluminum foil. Merck silica gel 60 was used as stationary phase for column chromatography. Celite® 545 was used for filtration. All the ^{1}H and ^{13}C NMR spectra were recorded on Bruker DRX 300 NMR spectrometer. Fluorescence emission spectra were recorded with a JASCO FP-6500 spectrometer and the slit width was 3 or 10 nm for excitation and 3 or 5 nm for emission. HRMS data were obtained from Agilent 6890 Series, with FAB positive

mode. Following figure is synthetic scheme for probes. (TEA = trimethylamine, Tf_2O = trifluoromethanesulfonic anhydride, dba = dibenzylideneacetone, BINAP = (±) 2,2'-bis(diphenylphosphino)-1,1'-binaphthyl, TFA = trifluoroacetic acid, DCM = dichloromethane.)

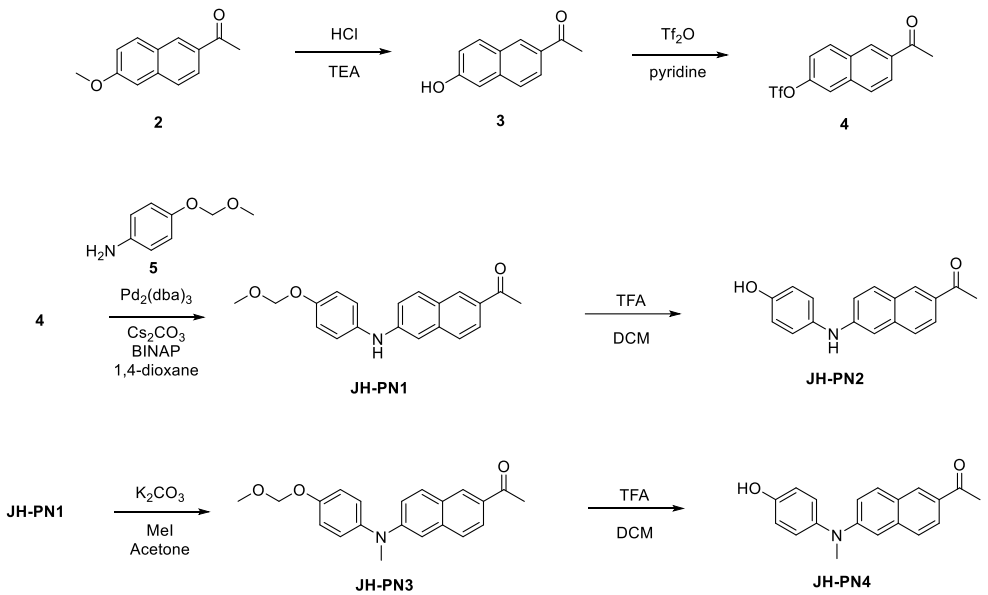

Compound **4** [5b] and **5** [8] were prepared by the literature method and synthesis of the other compounds is described below.

Synthesis of **JH-PN1**

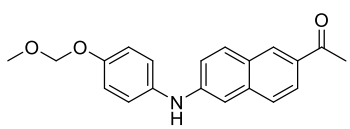

JH-PN1

A round bottom flask was charged with $Pd_2(dba)_3$ (0.05 equiv.), BINAP (0.15 equiv.) and Cs_2CO_3 (1.4 equiv.), and flushed with N_2 gas for 5 min. A solution of **4** (4.33 g, 13.6 mmol) and **5** (1.2 equiv.) in dioxane (10 ml) was added, and the resulting mixture was

first stirred under N_2 atmosphere at room temperature for 30 min and then at 100 ℃ for 20 h. At that time the reaction mixture was allowed to cool to room temperature, diluted with CH_2Cl_2 and filtered through a pad of Celite. The filter cake was washed with CH_2Cl_2. The filtrate was then concentrated and the residue was purified by silica gel column chromatography using CH_2Cl_2 as the eluent to give **JH-PN1** in 63.4% yield. ^{1}H NMR (300 MHz, $CDCl_3$): δ 8.35 (s, 1H), 7.89 (dd, J = 38.3, 7.7 Hz, 2H), 7.61 (d, J = 8.2 Hz, 1H), 7.22 – 7.10 (m, 6H), 5.89 (s, 1H), 5.21 (s, 2H), 3.55 (s, 3H), 2.70 (s, 3H); ^{13}C NMR (75.47 MHz, $CDCl_3$): δ 197.81, 153.68, 145.41, 137.55, 135.35, 131.64, 131.09, 130.24, 127.02, 126.35, 124.79, 123.29, 119.11, 117.48, 107.38, 94.91, 56.04, 26.50. HRMS (FAB^+) [M=$C_{20}H_{19}NO_3$], calculated 321.1365, found 321.1365.

Synthesis of **JH-PN2**

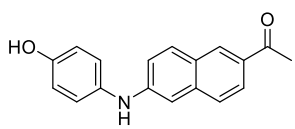

JH-PN2

To a solution of **JH-PN1** (321 mg, 1 mmol) in dry CH_2Cl_2 (5 ml), trifluoroacetic acid (5 ml) was added dropwise at 0 ℃. The resulting solution was stirred at room temperature until TLC indicated that all starting materials were consumed. The mixture was then concentrated in vacuo and azeotroped with toluene three times to give compound **JH-PN2**. The crude product was then purified by silica gel column chromatography using Hexane/EtOAc (4:1) as eluent to give **JH-PN2** in 99% yield. ^{1}H NMR (300 MHz, $CDCl_3$): δ 8.30 (s, 1H), 7.97 (dd, J = 19.5, 8.9 Hz, 2H), 7.50 (d, J = 8.9 Hz, 1H), 6.87 (d, J = 8.9 Hz, 2H), 6.63 – 6.56 (m, 4H), 5.77 (s, 1H), 4.83 (s, 1H),

2.66 (s, 3H); ^{13}C NMR (75.47 MHz, DMSO-d_6): δ 197.83, 153.76, 137.65, 136.27, 132.09, 131.07, 129.35, 128.85, 125.08, 124.98, 124.16, 123.99, 123.21, 116.33, 27.06. HRMS (FAB$^+$) [M= $C_{18}H_{15}NO_2$], calculated 277.1103, found 277.1103.

Synthesis of **JH-PN3**

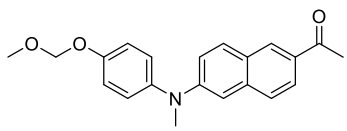

JH-PN3

JH-PN1 (406 mg, 1.263 mmol), methyl iodide (10 equiv.) and K_2CO_3 (3 equiv.) were stirred in acetone 20 ml at 60 ℃ for 2 days. The mixture was then concentrated in vacuo, diluted with CH_2Cl_2 and washed with water. The crude product was purified by silica gel column chromatography using Hexane/EtOAc (6:1) as eluent to give **JH-PN3** in 68% yield. ^{1}H NMR (300 MHz, $CDCl_3$): δ 8.34 (s, 1H), 7.95 (dd, J = 8.7, 1.62 Hz, 1H), 7.68 (dd, J = 18.3, 9.3 Hz, 2H), 7.22 – 7.04 (m, 6H), 5.21 (s, 2H), 3.55 (s, 3H), 3.41 (s, 3H) 2.69 (s, 3H); ^{13}C NMR (75.47 MHz, $CDCl_3$): δ 197.76, 154.88, 149.37, 142.18, 137.59, 131.34, 130.21, 130.15, 127.46, 126.41, 126.07, 124.66, 118.88, 117.55, 107.42, 94.70, 56.11, 40.75, 26.47. HRMS (FAB$^+$) [M= $C_{21}H_{21}NO_3$], calculated 335.1521, found 335.1521.

Synthesis of **JH-PN4**

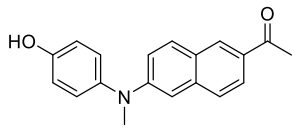

JH-PN4

To a solution of **JH-PN3** (335 mg, 1 mmol) in dry CH_2Cl_2 (5 ml), trifluoroacetic acid (5 ml) was added dropwise at 0 ℃. The resulting solution was stirred at room temperature until TLC indicated that all starting materials were consumed. The mixture was then concentrated in vacuo and azeotroped with toluene three times to give compound **JH-PN4**. The crude product was then purified by silica gel column chromatography using Hexane/EtOAc (4:1) as eluent to give **JH-PN4** in 99% yield. ^{1}H NMR (300 MHz, $CDCl_3$): δ 8.32 (s, 1H), 7.95 (dd, J = 10.3, 7 Hz, 1H), 7.67 (dd, J = 19.7, 10.6 Hz, 2H), 7.16 – 6.89 (m, 6H), 4.78 (s, 1H), 3.40 (s, 3H), 2.66 (s, 3H); ^{13}C NMR (75.47 MHz, DMSO-d_6): δ 198.15, 153.63, 149.613, 141.06, 137.67, 131.16, 130.33, 130.17, 127.97, 126.37, 125.91, 124.66, 118.64, 116.61, 106.98, 40.76, 26.44. HRMS (FAB^+) [M= $C_{19}H_{17}NO_2$], calculated 291.1259, found 291.1259.

Two-Photon Fluorescence Microscopy.

The two-photon fluorescence microscopy images were obtained with a DMI6000B Microscope (Leica) by exciting the probes with a mode-locked titanium-sapphire laser source (Mai Tai HP; Spectra Physics, 80 MHz pulse frequency, 100 fs pulse width)set at wavelength 740 nm and output power 2679 mW, which corresponded to approximately 1.5 mW average power in the focal plane.

Measurement of Two-Photon Cross Section.

The two-photon cross section (δ) was measured with femtosecond (fs) fluorescence measurement technique as described.[9] Rhodamine 6G was used as the reference. The intensities of the two-photon excited fluorescence spectra of the reference and sample were obtained at the same excitation wavelength. The TPA cross section was calculated by using $\delta = \delta_r(S_s\Phi_r\varphi_r c_r)/(S_r\Phi_s\varphi_s c_s)$: where the subscripts s and r stand for the sample and reference molecules. The intensity of the signal collected by a CCD detector was denoted as S. Φ is the fluorescence quantum yield. φ is the overall fluorescence collection efficiency of the experimental apparatus. The number density of the molecules in solution was denoted as c. δ_r is the TPA cross section of the reference molecule.

Cell Culture.

All cells were plated on glass-bottomed dishes (NEST) before imaging for two days. They were maintained in a humidified atmosphere of 5/95 (v/v) of CO_2/air at 37 ℃. The cells were incubated with **JH-PN4** at 37 ℃ under 5 % CO_2 for 30 min, washed three times with phosphate buffered saline (PBS; Gibco), and then imaged. The culture mediums for Raw 264.7 cells (ATCC, Manassas, VA, USA): DMEM (WelGene Inc, Seoul, Korea) supplemented with 10 % FBS (WelGene), penicillin (100 units/ml), and streptomycin (100 μg/mL).

B.1.5. Reference

[1] Jou, M. J.; Jou, S. B.; Guo, M. J.; Wu, H. Y.; Peng, T. I. *Ann. N. Y. Acad. Sci.* **2004**, *1011*, 45.

[2] Helmchen, F.; Denk, W. *Nat. Methods*, **2005**, *2*, 932–940.

[3] (a) Kim, H. M.; Cho, B. R. *Acc. Chem. Res.* **2009**, *42*, 863–872; (b) Yao, S.; Belfield, K. D. *Eur. J. Org. Chem.* **2012**, 3199–3217; (c) Liu, F.; Wu, T.; Cao, J.; Cui, S.; Yang, Z.; Qiang, X.; Sun, S.; Song, F.; Fan, J.; Wang, J. ; Peng, X.; *Chem. – Eur. J.* **2013**, *19*, 1548–1553; (d) Li, L.; Zhang, C. W.; Chen, G. Y.; Zhu, B.; Chai, C.; Xu, Q. H.; Tan, E. K.; Zhu, Q.; Lim, K. L.; Yao, S. Q. *Nat. Commun.* **2014**, *5*, 3276; (e) Dong, X.; Heo, C. H.; Chen, S.; Kim, H. M.; Liu, Z. *Anal. Chem.* **2014**, *86*, 308–311; (f) Zhou, L.; Zhang, X.; Wang, Q.; Lv, Y.; Mao, G.; Luo, A.; Wu, Y.; Wu, Y.; Zhang, J.; Tan, W. *J. Am. Chem. Soc.* **2014**, *136*, 9838–9841.

[4] (a) Lee, H.W.; Heo, C. H.; Sen, D.; Byun, H. O.; Kwak, I. H.; Yoon, G.; Kim, H. M. *Anal. Chem.* **2014**, *86*, 10001–10005; (b) Li, L.; Shen, X.; Xu, Q. H.; Yao, S. Q. *Angew. Chem., Int. Ed.* **2013**, *52*, 424–428; (c) Li, L.; Ge, J.; Wu, H.; Xu, Q. H.; Yao, S. Q. *J. Am. Chem. Soc.* **2012**, *134*, 12157–12167.

[5] (a) Li, X.; Tao, R.; Hong, L.; Cheng, J.; Jiang, Q.; Lu, Y.; Liao, M.; Ye, W.; Lu, N.; Han, F.; Hu, Y.; Hu, Y. *J. Am. Chem. Soc.* **2015**, *137*, 12296-12303; (b) Peng, T.; Wong, N.; Chen, X.; Chan, Y.; Ho, D.H.; Sun, Z.; Hu, J.J.; Shen, J.; El-Nezami, H.; Yang, D. *J. Am. Chem. Soc.* **2014**, *136*, 11728−11734

[6] (a) Kim, H. M.; Seo, M. S.; An, M. J.; Hong, J. H.; Tian, Y. S.; Choi, J. H.; Kwon, O.; Lee, K. J.; Cho, B. R. *Angew. Chem., Int. Ed.* **2008**, *47*, 5167.; (b) Rao, A. S.; Kim, D.; Nam, H.; Jo, H.; Kim, K. H.; Ban, C.; Ahn, K. H. *Chem. Commun.* **2012**, *48*, 3206.; (c) Rao, A. S.; Kim, D.; Wang, T.; Kim, K. H.; Hwang, S.; Ahn, K. H. *Org. Lett.* **2012**, *14*, 2598.; (d) Kim, H. M.; An, M. J.; Hong, J. H.; Jeong, B. H.; Kwon, O.; Hyon, J. Y.; Hong, S. C.; Lee, K. J.; Cho, B. R. *Angew. Chem., Int. Ed.* **2008**, *47*, 2231.

[7] Zhang, Q.; Zhang, N.; Long, Y.; Qian, X.; Yang, Y. *Bioconjugate Chem.* Article ASAP, DOI: 10.1021/acs.bioconjchem.5b00396

[8] Rejca, L.; Fabrisa, J.; Adrovića, A.; Kasuniča, M.; Petrič, A. *Tetrahedron Lett.* **2014**, *55*, 1218-1221

[9] Lee, S. K.; Yang, W. J.; Choi, J. J.; Kim, C. H.; Jeon, S. J.; Cho, B. R. *Org. Lett.* **2005**, *7*, 323.

B.2. Lanthanide-based Two-Photon Probes for Peroxynitrite

B.2.1. Introduction

Two-photon excitable lanthanide complexes have been developed and have shown the possibility of sensitization of the lanthanide with two-photon excitable sensitizer. [1,2,3,4,5] Some of the lanthanide complexes succeeded in penetrating the cells. [6,7,8] However, these probes are just for imaging the cell and not for detecting any specific target. Many groups have tried to develop a lanthanide-based two-photon probe that detects a specific target for biomedical application. Because it can offer advantages to both the two-photon probes and lanthanide-based probes. The advantages such as localized excitation, reduced photodamage, longer observation time, and greater tissue penetration depth, show sharp, line-like emission bands whose wavelengths are same with various environments and long excited state life time allowing time-resolved spectroscopy which can eliminate interferences that are caused by scattering and autofluorescence in biological conditions. However, this has not been developed. Therefore we designed and synthesized the lanthanide-based two-photon excitable complex for detecting peroxynitrite.

B.2.2. Results and Discussion

Design of Probes

We designed **Tb-PN** and **Eu-PN** with modification of **JH-PN4** in section B.1. **JH-PN4** was used as sensitizer of lanthanides and a targeting moiety. (Figure 1) When the N-phenyl group, the quencher, is dearylated by $ONOO^-$, the excited state of the sensitizer (acedan) can go through an intersystem crossing according to the heavy atom effect by lanthanide. Then, the energy transfer from the resulting triplet excited state to the lanthanide can occurs. Therefore, two-photon excited lanthanide phosphorescence can be detected.

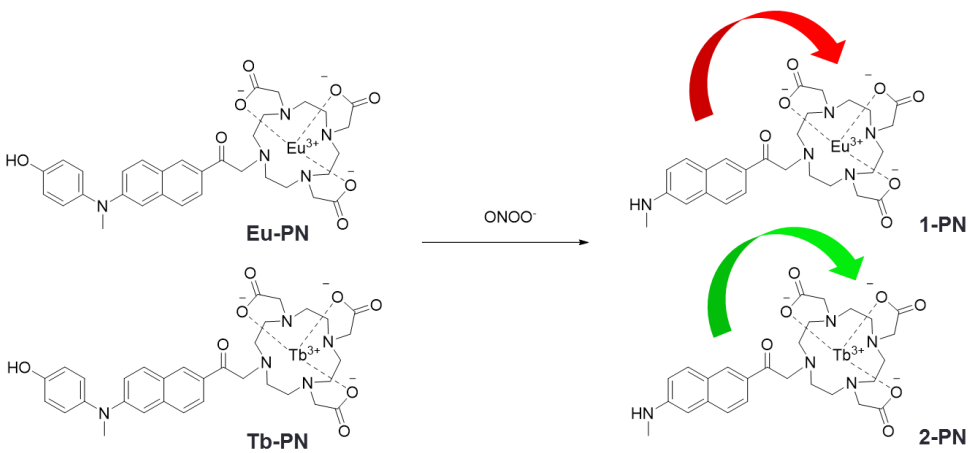

Figure 1. Design of probes

Luminescence responses of probes

We tested the luminescence responses of probes to $ONOO^-$ in order to confirm whether the sensitization from **JH-PN4** to lanthanide occurs. 2 equiv. of ONOO- was added to the probe in 10 mM PBS solution (0.4% DMF, pH 7.4). However, expected responses were not observed. **Tb-PN** showed no luminescence with or without $ONOO^-$. **Eu-PN** showed the only detectable turn-on response with 2 equiv. of $ONOO^-$. (Figure 2)

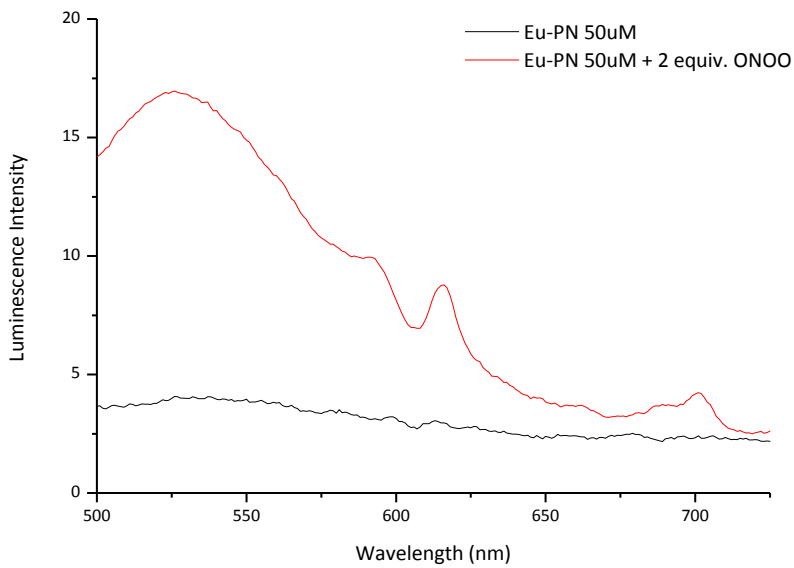

Figure 2. Luminescence spectra of **Eu-PN** (50 μM) with 2.0 equiv. of $ONOO^-$. Data were acquired at 25 ℃ in 10 mM phosphate buffer (0.4% DMF) at pH 7.4 with excitation at 400 nm. Reaction were carried out for 1h at room temperature before the fluorescence intensity of the probe solution was measured.

To explain these results, we observed phosphorescence of **Eu-PN** (50 μM) with 2.0 equiv. of $ONOO^-$. (Figure 3) Phosphorescence from the triplet excited state of sensitizer was a major part of the phosphorescence spectra and a minor phosphorescence of europium emission was observed. Through a maximum emission wave length of the sensitizer, we could calculate the energy level of triplet excited state of sensitizer (19230 cm^{-1}). Because the energy level of the triplet excited state (19230 cm^{-1}) is smaller than that of the emissive excited state of Tb^{3+} (20490 cm^{-1}). Thus, sensitization cannot occur resulting no luminescence of terbium. Otherwise, the energy level of the emissive excited state of Eu^{3+} was smaller than that of the sensitizer. The energy difference is greater than 1850 cm^{-1}, which means that sensitization is possible.[9]

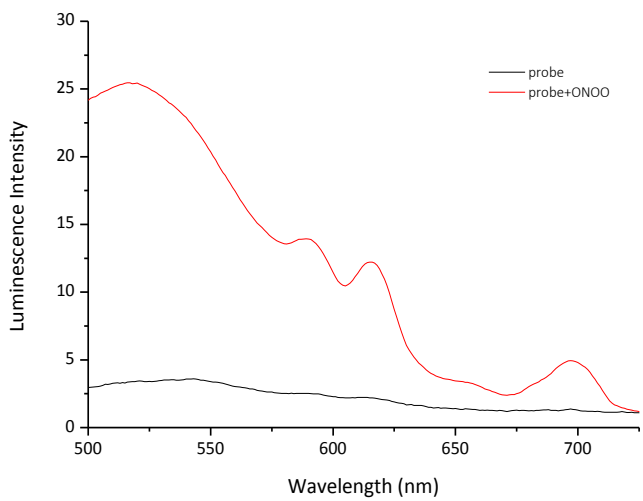

Figure 3. Phosphorescence spectra of **Eu-PN** (50 μM) with 2.0 equiv. of $ONOO^-$. Data were acquired at 25 ℃ in 10 mM phosphate buffer (0.4% DMF) at pH 7.4 with excitation at 400 nm, dealay time = 2 ms. Reaction were carried out for 1h at room temperature before the fluorescence intensity of the probe solution was measured.

However, the energy difference was so small (1990 cm^{-1}) that sensitization cannot occur efficiently. As a result, only a very weak emission of Eu^{3+} is observed. (Figure 2, 3)

B.2.3. Conclusion

We designed and synthesized the lanthanide-based two-photon probe detecting peroxynitrite. However, the energy level of the triplet excited state of the sensitizer was too low to sensitize the lanthanide. Therefore, the sensitizer should be changed to another sensitizer with higher energy level of the triplet excited state to develop lanthanide based two-photon probe. In addition, targeting moiety also should be changed because of low reactivity. Further studies for developing new probes for other targets using 6-(benzo[d]oxazol-2-yl)-2-(N, N-dimethylamino) naphthalene (BODAN)[10] as fluorophore is ongoing.

B.2.4. Experimental Section

Synthesis and characterization of probes

All the chemicals were purchased from commercial suppliers and used without further purification except anhydrous solvents. Reactions were monitored by thin layer chromatography with Merck silica gel 60 F254 on aluminum foil. Merck silica gel 60 was used as stationary phase for column chromatography. Celite® 545 was used for filtration. All the ^{1}H and ^{13}C NMR spectra were recorded on Bruker DRX 300 NMR spectrometer. Fluorescence emission spectra were recorded with a JASCO FP-

6500 spectrometer and the slit width was 3 or 10 nm for excitation and 3 or 5 nm for emission. HRMS data were obtained from Agilent 6890 Series, with FAB positive mode. Following figure is synthetic scheme for probes. (LiHMDS = lithium bis(trimethylsilyl)amide, THF = tetrahydrofuran, ACN = acetonitrile, TFA = trifluoroacetic acid, DCM = dichloromethane, MeOH = methanol.)

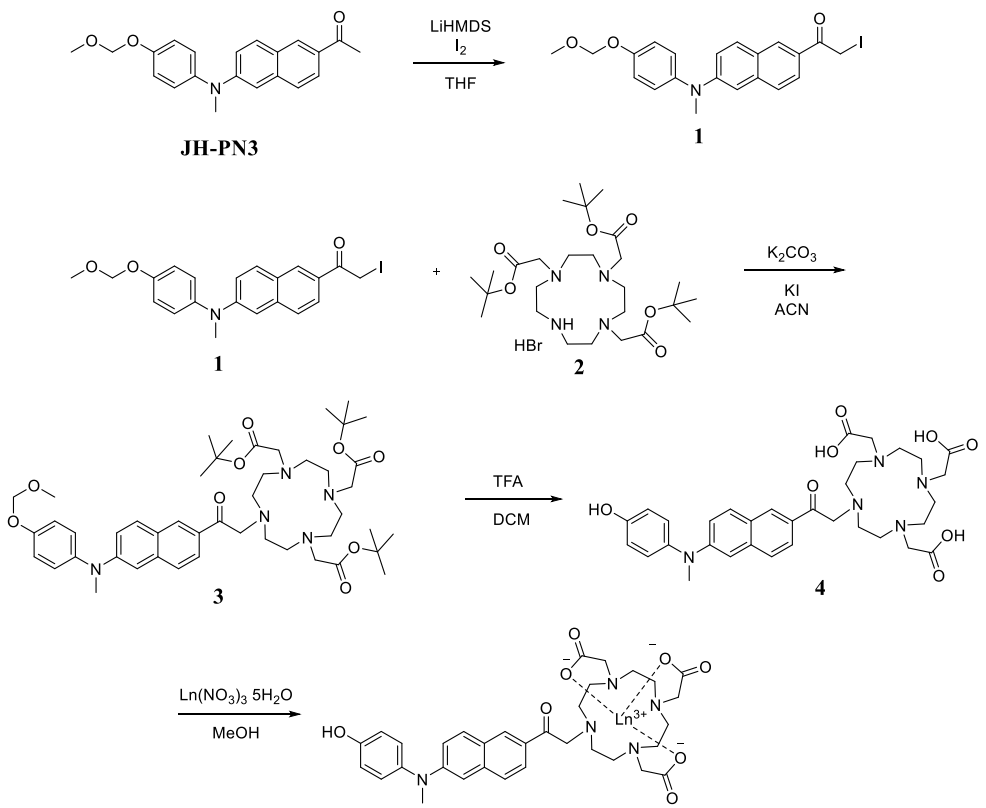

Ln = Eu (**Eu-PN**), Tb (**Tb-PN**)

Compound **JH-PN3** (see section B.1.4) and **3** [11] was prepared by the literature method and synthesis of the other compounds is described below.

Synthesis of **1**

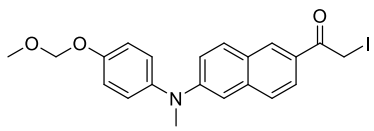

1

JH-PN3 (320 mg, 0.954 mmol) was dissolved in dry THF (5 ml) under N_2. LiHMDS (1.0 M in THF, 1.3 ml) was added dropwisely to **JH-PN3** solution at -78 °C in dark. After stirring 30 min, I_2 (242 mg, 0.954 mmol) in THF (5 ml) was added dropwisely over 5 min to solution. After stirring 30 min, the temperature was changed to 0 °C and the reaction was quenched with 1 M $NaHSO_4$ (2 ml), water (5 ml) and ether (30 ml). The mixture was washed twice with $Na_2S_2O_3$ and water and brine. And then, it was concentrated in vacuo and purified by silica gel column chromatography using Hex/EtOAc (6:1) as eluent to give **1** in 93% yield. ^{1}H NMR (300 MHz, $CDCl_3$): δ 8.37 (s, 1H), 7.94 (d, J = 8.57, 1H), 7.69 (dd, J = 19.97, 0 Hz, 2H), 7.21 – 7.03 (m, 6H), 5.23 (s, 2H), 4.46 (s, 2H), 3.55 (s, 3H), 3.42 (s, 3H); ^{13}C NMR (75.47 MHz, $CDCl_3$): δ 192.36, 155.06, 149.77, 141.92, 137.95, 131.01, 130.36, 127.62, 127.35, 126.70, 125.93, 125.16, 118.91, 117.59, 107.19, 94.69, 56.14, 42.16, 40.77, 2.13.

Synthesis of **3**

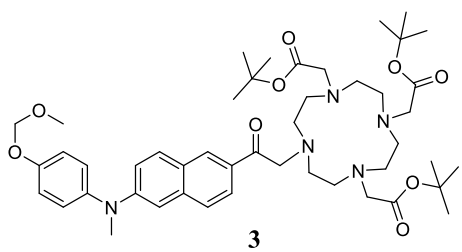

3

1 (400 mg, 0.867 mmol), **2** (0.9 equiv.) and K_2CO_3 (3 equiv.) is dissolved in Acetonitrile 10 ml and refluxed at 60 °C. After stirring overnight, the mixture was concentrated in vacuo. And then, it was worked up with CH_2Cl_2, MeOH and water. The crude product was purified by silica gel column chromatography using CH_2Cl_2/MeOH (100:1 to 20:1) as eluent to give **1** in 70% yield. ^{1}H NMR (300 MHz, $CDCl_3$): δ 8.27 (s, 1H), 7.81 (d, J = 8.66, 1H), 7.65 (dd, J = 24.81, 7.65 Hz, 2H), 7.19 – 6.99 (m, 6H), 5.20 (s, 2H), 4.08 (s, 2H), 3.53 (s, 3H), 3.40 (s, 3H), 3.40 – 2.10 (m, 22H), 1.49 – 1.27 (m, 27H) ; ^{13}C NMR (75.47 MHz, $CDCl_3$): δ 198.55, 172.76, 155.03, 149.55, 141.90, 137.87, 130.20, 129.65, 129.40, 127.60, 126.47, 125.80, 123.83, 118.77, 117.57, 107.00, 94.70, 81.99, 81.90, 77.29, 59.97, 56.11, 55.86, 55.66, 40.73, 27.34, 27.85.

Synthesis of **Ln-PN**

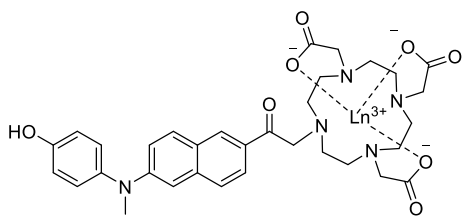

Ln = Eu (**Eu-PN**), Tb (**Tb-PN**)

3 (20 mg, 0.0236 mmol) was dissolved in CH_2Cl_2 (0.5 ml). CH_2Cl_2 (0.5 ml) and TFA (0.5 ml) was added dropwisely at 0 °C to make CH_2Cl_2/TFA (2:1) solution. After stirring overnight, the mixture was concentrated in vacuo. And then, the **4** was made in 98.6% yield. **4** is used without further purification; **4** and $Ln(NO_3)_3.5H_2O$ (1.2 equiv.) was dissolved in MeOH/H_2O (2:3) solution and refluxed for 2days at 60 °C. And then, acetone was poured to precipitate and the precipitation was filtered to be purified. The product **Ln-PN** is made in 54.8~60% yield.

Eu-PN in 54.8% yield. HRMS (FAB^+) [M= $C_{33}H_{38}EuN_5O_8$], calculated 786.2011, found 786.2014. UV−vis (H_2O) λ max (ε /M−1 cm−1): 260 nm (9048), 300 nm (3428), 421 nm (3944).

Tb-PN in 60% yield. HRMS (FAB^+) [M= $C_{33}H_{38}N_5O_8Tb$], calculated 792.2052, found 786.2052. UV−vis (H_2O) λ max (ε /M−1 cm−1): 256 nm (5218), 302 nm (2094), 394 nm (1912).

B.2.5. Reference

[1] Piszczek, G.; Maliwal, B. P.; Gryczynski, I.; Dattelbaum, J.; Lakowicz, J. R. *Journal of Fluorescence*, **2011**, *11*, 101-107

[2] Picot, A.; Malvolti, F.; Guennic, B. L.; Baldeck, P. L.; Gareth Williams, J. A.; Andraud, C.; Maury O. *Inorg. Chem.* **2007**, *46*, 2659-2665

[3] Hao, R.; Li, M.; Wang, Y.; Zhang, J.; Ma, Y.; Fu, L.; Wen, X.; Wu, Y.; Ai, X.; Zhang, S.; Wei, Y. *Adv. Funct. Mater.* **2007**, *17*, 3663–3669

[4] Fu, L.; Wen, X.; Ai, X.; Sun, Y.; Wu, Y.; Zhang, J.; Wang, Y. *Angew. Chem. Int. Ed*. **2005**, *44*, 747 –750

[5] D'Ale´o, A.; Picot, A.; Baldeck, P. L.; Andraud, C.; Maury, O. *Inorg. Chem.* **2008**, *47*, 10269-10279

[6] Picot, A.; D'Ale´o, A.; Baldeck, P. L.; Grichine, A.; Duperray, A.; Andraud, C.; Maury, O. *J. Am. Chem. Soc.* **2008**, *130*, 1532-1533.

[7] Eliseeva, S.V.; Aubo¨ck, G.; Mourik, F. V.; Cannizzo, A.; Song, B.; Deiters, E.; Chauvin, A.; Chergui, M.; Bu¨ nzli, J. G. *J. Phys. Chem. B*, **2010,** *114*, 2932–2937

[8] Lo, W.; Kwok, W.; Law, G.; Yeung, C.; Chan, C. T.; Yeung, H.; Kong, H.; Chen, C.; Murphy, M. B.; Wong, K.; Wong, W. *Inorg. Chem*. **2011**, *50*, 5309–5311

[9] Latva, M.; Takalo, H.; Mukkala, V.-M.; Matachescu, C.; Rodriguez-Ubis, J.C.; Kankare, J.; *J. Lumin*. **1997**, *75* ,149.

[10] Rathore, K.; Lim, C. S.; Lee, Y.; Cho, B. R. *Org. Biomol. Chem.* **2014**, *12*, 3406

[11] Prasuhn, D. E.; Yeh, R. M.; Obenaus, A.; Manchester, M.; Finn, M. G. *Chem. Commun*. **2007**, 1269 –1271.

국문 초록

이광자 분광법은 근적외선 영역의 광자 2 개를 여기원으로 이용하는 것으로 생의학 연구의 유용한 도구로 사용되어 왔다. 그러나 이광자 여기가 가능한 과산화 아질산염에 대한 프로브는 현재까지 극소수만이 개발되어왔다. 현재까지 개발된 프로브들은 다양한 생물학적 환경에서 이광자 분광법을 이용하여 과산화 아질산염을 감지할 수 있지만, 과산화 아질산염에 대한 탐구를 더 진행하기 위해서는 개선된 이광자 흡수성을 보이는 프로브가 개발되어야 한다.

우리는 탈아릴화 반응을 이용해서 다른 활성 산소 종, 활성 질소 종들 가운데서 선택적으로 과산화 아질산염만을 감지하는 새로운 프로브를 개발하였다. 개발된 프로브는 과산화 아질산염에 높은 선택성과 감도를 가지며, 이전에 발표된 프로브들보다 더 나은 이광자 흡수성을 가진다.

여기서 더 나아가 우리는 란탄족 원소의 인광이 가지는 독특한 특징들을 도입하기 위해 이광자 여기가 가능한 란탄족 원소 복합체를 합성하였다. 추가적인 개선을 통해 이 란탄족 원소 기반의 이광자 프로브들은 아직 명확하게 밝혀지지 않은, 생물계에 존재하는 과산화 아질산염의 효과들을 발견하는 것에 사용될 수 있다.

주요단어 : 과산화 아질산염, 이광자 분광법, 형광 프로브, 란탄족 원소 복합체

학번 : 2013-22923